Development of calibration equations for capacitance sensors to measure soil water content using an IoT-based network

by

Prabakaran Santhanam

A thesis submitted to the Faculty of Graduate Studies of

The University of Manitoba

in partial fulfilment of the requirements of the degree of

MASTER OF SCIENCE

Department of Biosystems Engineering

University of Manitoba

Winnipeg, Canada

ABSTRACT

Soil Water Content (SWC) plays a vital role in agriculture. Knowledge of SWC helps the farmers understand the crop's water requirement and achieve a better yield. Due to commercialization, well-developed sensors are expensive for large-scale agriculture. There is a need for low-cost soil sensors to measure SWC precisely with spatial and temporal resolution. Low-cost soil sensors like SEN0193 needed to be calibrated and validated using the gravimetric method to obtain SWC. The SEN0193 sensors were integrated with the raspberry-pi stand-alone system, with mini-controllers (Arduino) to log the data from the sensors. The SEN0193 sensors were tested under a controlled environment with target VWC samples (Sand: 10, 20, 25, 30%, Loam: 10, 20, 30, 40, 50%, Clay: 10, 20, 30, 40%) prepared in the laboratory. The calibration equations were developed and validated both under laboratory and field conditions to find out the accuracy and precision. The SEN193 sensors demonstrated poor precision on fine particle-sized soils such as loam (0.003 m^3/m^3) and clay (0.003 m^3/m^3) and moderate precision on sand (0.002 m^3/m^3). Validation of sensors at different depths of 20 cm and 40 cm during the field study proved that the surface contact of the sensor with soil was affected by the air gap. Each sensor provided a different precision, which confirms the SEN0193 sensor's fragile nature. A comparison of TEROS T10 sensors with SEN0193 sensors showed that the T10 sensors work with better accuracy and precision. Monitoring the airgap is, a better installation method with careful handling of the SEN0193 sensor could increase its performance. A water uptake pattern study of the canola root zone was conducted using the SEN0193 sensor at the Winkler site. Rainfall and the presence of crops influenced the upward groundwater flux. The shallow groundwater table with saline content adversely affects the crop. Using the sub-surface drainage system to remove the excess water will help the crop to attain a higher yield by limiting the upward flux of saline groundwater.

Ackonwledgments

Firstly, I would like to express my sincere gratitude to Dr. Sri Ranjan for his constant support, invaluable advice, and patience during my entire master's degree period. His vast knowledge and wealth of experience have motivated me throughout my academic career and daily life.

I dedicate immerse thanks to Dr. Jason Morrison for his tireless help with the data analysis on the research and for being one of the committee members. I would also extend my sincere thanks to Dr. Greg E. Bridges for his constant help and support as a committee member.

I sincerely appreciate Mr. Dale Bourns, Mr. Matt McDonald's, and Mr. Kerry Lynch's efforts in fabrication and technical support.

I appreciate the Natural Sciences and Engineering Research Council (NSERC) for supporting my studies. I am thankful for the funding provided by the Faculty of Graduate Studies and the Graduate Student Association at the University of Manitoba to enable me to present my work at conferences.

I sincerely thank Dr. Emeka Ndulue for sharing the sensors that provided the basis of the study that served as the foundation for my thesis. I want to express my gratitude to Mr. Krishna Phani Kaja and Ms. Thushyanthy Akilesan for helping me focus by encouraging me and sharing their insights during my education. I would like to mention Mr. Divagar Vakeesan and Ms. Darsana Divagar for their constant support and help with every situation and took care like a brother. I owe huge thanks to Ms. Poorany William for her motherly caring and kindness during my entire study period.

I deeply acknowledge and thank my friends Narendran Ramasamy Boopathy, Akilesan Vamadevan, Vimala Bharathi S K, Lavanya Ganesan, Raghu Ram Atmuri, and Vignesh Rajendran, and other friends for their help and support.

Dedication

This thesis is dedicated to my mother and my father for always being with me

Devotions to

Muruga

Love you

Manikandan - Varsha

Thoushika Sri

Thanks

Amma – Appa

Ramanathan Sri Ranjan

TABLE OF CONTENTS

LIST OF FIGURES

LIST OF TABLES

Acronyms

ADC	Analog to Digital Converter
IDE	Integrated Development Environment
IoT	Internet on Things
MBE	Mean Bias Error
MAE	Mean Absolute Error
R^2	Regression Coefficient
RMSE	Root Mean Square Error
SWC	Soil Water Content
TTL	Transistor-Transistor Logic
TDR	Time Domain Reflectometer
VWC	Volumetric Water Content

1.0 Introduction

1.1 Problem statement

In sustainable crop water management, Soil Water Content (SWC) needs to be monitored with accurate temporal & spatial resolution. Knowledge in SWC helps us to achieve high water application efficiencies and to obtain better yields. Especially in a sub-irrigation system, continuous monitoring of soil moisture status leads to the use of groundwater in the most efficient way. The use of groundwater as an alternative irrigation source has been overlooked, and the research on this is minimal. Continuous soil water monitoring inside and below the crop rooting zone can be used to estimate evapotranspiration during periods of low water redistribution from the root zone. Many sources of data are available to assist farmers in making the right irrigation decision. Meteorological data, assessed and predicted, include temperature, relative humidity, precipitation, radiation, and wind speed. The status of soil water in the soil matrix or SWC gives farmers data to determine how much water the crop needs to grow. The irrigation needs of the plants can be determined by direct & indirect methods that have been used over the past 30 years. The traditional gravimetric method is the most common & simplest method used in the system to find the Volumetric Water Content (VWC) of the soil. Still, it is quite a labor-intensive and time-consuming technique. Resistive type gypsum block method, heat dissipation, piezometers, and tensiometers were used to measure the soil water potential, which requires complex-data analysis. In electromagnetic techniques such as time domain reflectometry, frequency domain reflectometry is commonly used because of its ease of use. Although many techniques are available, the most accurate and precise way of measuring SWC is yet to be determined.

In the past decade, numerous industries and researchers have been interested in developing SWC sensors. As a result, there is an abundant invention of new sensors, and most newly

developed sensors are based on the principle of capacitance and resistance. However, these sensors are expensive because of their commercialization. They are not suitable for large-scale farms since they need to be calibrated. Some of the sensors have their factory calibration. An excellent sensor should be capable of easy installation and operation and provide accurate, precise, and easy-to-interpret data.

With the rapid development of technology, sensors can transmit data using Wireless Sensor Networks (WSNs), which leads to real-time data monitoring like smart farming. The arrival of the Internet of Things (IoT) enables the most elegant way of data acquisition and interpreting the obtained data to make a better decision without any delay. These IoT instruments are relatively cheap and can easily integrate with sensors.

During the summer of 2020, we conducted a field study to evaluate the performance of low-cost capacitance soil moisture sensors (SEN0193) using a calibration equation developed in our laboratory study. In the laboratory, sensors were tested with soil samples prepared at a range of target moisture contents using the gravimetric method under controlled conditions. SEN0193 sensors are connected to a microcontroller (Arduino) and integrated with Raspberry Pi to get continuous VWC data, which can be accessed remotely using a wireless module. The traditional gravimetric method and well-developed commercial TEROS T10 (Meter Environment) sensor were used to compare the results obtained from the SEN0193 sensor. Based on the sensor's behavior on different soil types from the laboratory studies, the field study was conducted in a more similar soil. In the year 2021 summer season field study was carried out on canola crops to study their root water uptake behavior using the developed calibration equations.

1.2 Scope

Using factory-calibrated high-cost soil moisture sensors limits the possibility of measuring VWC with good spatial & temporal resolution. In large-scale farming, the number of sensors will be less, as will the moisture content data. The heterogeneous nature of soil leads to monitoring VWC in each layer of the soil to find the accurate VWC. The study focuses on using low-cost soil moisture sensors to monitor the VWC & enable continuous data collection without disturbing the soil much compared to other methods available in the system. Since SEN0193 sensors do not have their factory calibration, there is a need to develop the calibration equation for major texture types of soil.

Objectives

The main objective of the study was to develop the calibration equation and evaluate the performance of the low-cost SEN0193 sensors under controlled soil moisture conditions in the laboratory and the field. The specific objectives were to:

1. Developing the calibration equation for three major soil texture types under laboratory conditions.
2. Validating the calibration equation in the field and comparing the sensor performance against a commercial TEROS T10 (Meter Environment) sensor.
3. Use the sensor to study the water root uptake pattern of canola in the field.

1.3 Outline of thesis

This thesis consists of six chapters. The first chapter focuses on the overview and importance of soil moisture measurement, the scope, and the objectives of the study. The second chapter describes a detailed literature review of previous studies on the SEN0193 sensor, the background theory of different soil moisture content measurement methods, the advantages of using the capacitance probes, the need for calibration equations in the indirect methods, and reviews on root water uptake behavior. The third chapter consists of materials used in the study and a detailed explanation of the preparation of sensors for the field study. The fourth chapter discusses the results from the study and performance of the sensors and the factors that affected the sensors' performance. The fifth chapter provides the conclusions about the outcomes of the experiments and highlights the recommendations for future study of the sensors.

2.0 Review of literature

2.1 Review of the SEN0193 sensor performance

With the increased abundance of commercial sensors, there is a growth in studies comparing selected sensors working under different principles. Information on the performance of capacitance-based soil moisture sensors on different soils remain sparse. Few studies on the capacitance soil moisture sensor (SEN0193) are available.

Radi et al. (2018) and Nagahage et al. (2019) evaluated the performance of SEN0193 sensors on a laboratory scale and developed their calibration equations using the gravimetric method as a standard. Radi et al. (2018) concluded that the SEN0193 sensors were affected by the environmental temperature conditions, but their performance showed a very good response in the local soils. Nagahage et al. (2019) evaluated the sensor's reliability and accuracy and they reported that these sensors did not perform well even under controlled conditions

Placidi et al. (2020) analysed the SEN0193 sensor's electric circuit characterization in detail. In that study, Placidi et al. (2020) found that the soil's compaction level (Porosity of soil) of the soil affects the sensor performance. These sensors provide highly correlated data with Gravimetric Water Content in a constant soil volume for a given soil texture. However, they tested the sensor on garden soils, organic soil samples, and silica sand. Both recommended conducting a field experiment to determine the sensor's full potential.

Ferrarezi et al. (2015) report that SEN0193 sensors are not waterproof and question their sensitivity to salinity. This research also focused on protecting the sensor's electrical circuitry, which is not waterproof. However, the present study involves field experiments to

measure VWC within the root zone and develop a universal calibration equation for the SEN0193 sensors used in major soil types.

2.2 Background Theory

2.2.1 Gravimetric Method

As explained by (Topp and Ferre 2002), the gravimetric method is the simplest and the most accurate way to find soil moisture content. It involves applying the simple mass balance equation given in Eq. 2.1.

$$\text{Gravimetric Water Content } (\theta_g) = \frac{\text{wet weight (g)} - \text{dry weight (g)}}{\text{dry weight (g)}} \quad (2.1)$$

The Volumetric Water Content (VWC) of soil is calculated using the dry bulk density of the soil and the dry and wet mass of the soil. The sample's dry bulk density (ρ_b) was calculated using the following equation given in Eq. 2.2. Volume of the soil can be calculated from the surface area of the container (A) and the height of dry soil filled in the container (cm) using the Eq. 2.3.

$$\rho_b = \frac{m_s}{V} \quad (2.2)$$

$$V = A \times h \quad (2.3)$$

Where:

m_s = mass of the dry in the container (g)

V = total volume of the soil (cm^3)

A = surface area of the container (cm^2)

h = height of dry soil filled in the container (cm).

Soil samples steadily decline in mass over several days at 105°C. The organic compounds present in soil samples can be volatile at 105°C, which can result in decreased mass because of the volatilization of other elements. This method was originally adopted by Gardner (1986). The oven-drying method is a widely used and convenient method of obtaining a good estimate of the soil water content.

Topp and Ferre (2002) recommend using more than two methods to compare results while performing calibrations because of the destructive nature of sampling. Errors arise while converting GWC to VWC in salt-affected soils, as also some other uncertainties like oven temperature, air degree, flow, and drying time (Topp and Ferré 2002).

2.2.2 Tensiometer Method

The tensiometer method works under the principle of soil water potential. Buckingham (1907) developed this method and, a soil water potential instrument later named a Livingston (1908) tensiometer. This instrument monitors the energy status of the soil solutions known as soil water potentials (Soil Science Society of America [SSSA], 1997). The soil water potential is generally described as the amount of energy per volume needed to extract water from the matrix (Nolz et al. 2013). The total Water Potential (ψ_t) of soil is modelled by dividing it into two parameters as the Water potential (ψ_w) and Gravitational potential (ψ_g) as shown in Eq. 2.4.

Total Water Potential (ψ_t) = Water potential (ψ_w) + Gravitational potential (ψ_g) (2. 2)

Where, Water potential is a sum of Pressure potential (ψ_p), Matrix potential (ψ_m), and Solute potential (ψ_s) as shown in Eq. 2.5

Water potential (ψ_w) = Pressure potential (ψ_p) + Matrix potential (ψ_m) + Solute potential (ψ_s) (2.5)

Wherever information on soil water is needed, a tensiometer can be used, beginning with putting a porous ceramic cup in the soil. Water is poured into the cup, the connecting tube, and the vacuum indicator detects the negative pressure. Through pores in the cup wall, the film of water in the soil around the cup makes hydraulic contact with the bulk water inside the cup. The cup water comes into hydraulic balance with the soil water as it flows in or out through the cup wall. The values on the tensiometer gauges fluctuate as soil water is drained by root activity or restored by rainfall or irrigation. Tensiometer readings displayed against time give a valuable record of soil water conditions in the surrounding region (Hanks 1992). Even though the tensiometers are well developed, they do not measure the entire soil water availability because of their limitation towards soil suction in an unsaturated condition. In such cases, pressure plate equipment is needed to calibrate resistance blocks or electrothermal units to measure soil suction. (Black & Gardner, 1965).

2.2.3. Electromagnetic methods

Electromagnetic methods use the flow of electrical current through a medium to measure the medium's electrical properties (Proulx 2001). In this method, the soil is considered a medium containing liquid within the space between soil particles. This resultant combination presents physical characteristics like compressibility, density, magnetic permeability, specific heat, dielectric permittivity, and electrical conductivity. Various commonly used and quickly growing

technologies for measuring soil water content are based on electromagnetism and may be traced back to Maxwell's equations for electric and magnetic field interactions (Topp and Ferré 2005). Using soil's electrical properties to measure VWC includes Time Domain Reflectometry (TDR), Capacitance devices, and Resistance sensors.

Time Domain Reflectometry is unlike conventional techniques of monitoring soil water content. Time-domain reflectometry (TDR) may be employed with minimum soil disturbance (Ju et al. 2010). The TDR can efficiently detect soil water content 1 m below the soil surface (Topp and Ferré 2005). The TDR measures the time it takes for an electromagnetic wave to travel along a waveguide. The travel time of the electromagnetic step-pulse through the soil medium it is buried in is determined by the reflection of the pulse at the end of the TDR probe (Yu et al. 2010) (Adelakun 2013). The wave shape is used to calculate the wave's propagation velocity across the medium. The dielectric constant of the medium surrounding the TDR probes may be used to calculate the propagation velocity. Using the given (Eq. 2.6) Of Topp's equation (1980), an apparent dielectric constant (Ka) is used to indirectly compute the soil water content (Topp et al. 1980a).

$$\text{VWC } (\theta_v) = -5.3 \times 10^{-2} + 2.92 \times 10^{-2} K_a - 5.5 \times 10^{-4} K_a^{\,2} + 4.3 \times 10^{-6} K_a^{\,3} \qquad (2.6)$$

In Capacitance Devices, the soil serves as the capacitor's dielectric. (Topp and Ferre 2002) The alternating current field is generated by a running oscillator and gets adjusted to the capacitor to produce a tuned circuit. The resonance frequency is then calibrated to the dielectric permittivity, which is calibrated to the soil moisture content. The advantages of capacitance probes include ease of use, faster reaction times, safety, and accuracy when good soil-probe contact is established. They are automatic and can continuously log readings over wide areas and provide great resolution

of the soil profile. The capacitance probe readings affect the electrode design, the imposed frequency, and the apparent dielectric constant (Clarke Topp and Ferré 2002).

Resistance sensors are two non-connecting electrodes placed in a porous material that make up electrical resistance sensors (usually gypsum). A current is delivered between the two electrodes, and the resistance between the electrodes is influenced by VWC(θv); as VWC (θv) increases, the resistance between the electrodes decreases. A calibration equation may be used to convert the sensor's output voltage to soil matrix potential (m), which is proportional to the resistance in the porous medium. Electrical resistance sensors encased in gypsum blocks are susceptible to saline soil water and degrade quickly in salty and high-salinity environments (Rudnick et al. 2015) (Yoder et al. 1998).

2.3. Sensors based on the capacitance principle

Capacitance sensors were the most used technique to measure soil water content because they are amenable to automatic, continuous monitoring and ease of use. The arrival of IoT made these sensors easier to use in field study and for changing the default calibration curves for converting soil permittivity to soil water content, as well as irrigation scheduling (Topp and Ferré 2002). (Smith-Rose 1933) introduced the Capacitance-based sensor concept and rapidly evolved over a few years to a real-time monitoring system in the 1990s

Much research was carried out on this method over time. The advantages of capacitance probes include ease of use, faster reaction times, safety, and accuracy when good soil-probe contact is established. They are automatic and can continuously log readings over wide areas and provide great resolution of the soil profile. The capacitance probe readings affect the electrode design, the imposed frequency, and the apparent dielectric constant. As shown in Eq. 2.7, the relationship between the apparent dielectric constant and the total capacitance is

$$C = g\ \varepsilon ra \tag{2.7}$$

Where g is the geometric constant based on the configuration of the size, shape, and distance between the electrodes. Capacitance probes contain an inductor and capacitor linked to circuitry that oscillates at a frequency determined by the values of L and the electrode–soil capacitor. The frequency of oscillation is solely determined by changes in capacitance when L is constant (regulated by electronic circuitry). The capacitance is an inverse square root function of the oscillation frequency (F) as mentioned in Eq. 2.8.

$$F = \left(2\pi\sqrt{LC}\right)^{-1} \tag{2.8}$$

where L denotes total circuit inductance, and C represents total capacitance, which includes soil components and certain constants. (Gardner et al. 1998); (Proulx 2001); (Starr and Paltineanu 2002); (Evett et al. 2008); (Topp and Ferré 2005). The functional connection between oscillation frequency and soil water content for individual soils should be empirically determined by calibration as shown in Eq. 2.7.

$$F = f(\theta v) \tag{2.9}$$

Capacitance probes fulfil the soil moisture measurement needs in different crop root zones; the sensor probe may build according to the actual measurement depth. The profile soil moisture sensor offers a measuring accuracy of ±1.31 percent and excellent stability and consistency (Hua et al. 2016).

Fares et al. (2011) concluded that EC-10, EC-20, and ML2x probes demonstrated the greatest precision, because of their higher operating frequency under field conditions.

da Silva et al. (2018) stated that despite having a higher starting cost than the other sensors evaluated in this study, capacitance probes have acceptable acceptability due to the precision of the readings and the simplicity and speed of their use.

2.4. Need for Calibration equation

Commercialized, high-cost industry-developed soil moisture sensors have their factory-calibrated equations. However, those calibration equations were developed on soil type and in a particular site, which might not be ideal for all the types of soils and sites. The heterogeneous nature of soil limits applying a common equation to calculate the VWC. It is essential that specific site calibration need to be carried out (Yoder et al. 1998).

Rowlandson et al. (2013) recommended that taking soil texture into account, either by generating separate calibration equations based on soil texture categories or by developing calibration equations based on plant land cover, gave the lowest RMSE values. According to research by Iwata et al. (2017), the calibration of repacked soil columns differs from that of disturbed soil utilized in laboratory studies.

Hignett and Evett (2008) specify that a manufacturer's sensor calibration is usually done in a temperature-controlled chamber with distilled water and easy-to-handle homogenous soil components (loams or sands) uniformly packed around the sensor. This results in a highly exact and accurate calibration for the conditions being tested. However, in the field, variables such as rocks, roots, level of clay content, temperature, soil compaction, and salinity frequently render the manufacturer's calibration ineffectual (Hignett and Evett 2008). A calibration equation correlates the probe's output period to soil water content (Ruelle and Laurent 2008). the difference in the type of soil influences the soil moisture sensor's readings, hence there is a need to calibrate

the sensors for each soil type and texture. The calibration of a sensor for one soil texture type may not be suitable for another type of soil. This research covers the three major texture types such as sand, loam, and clay.

2.5. Importance of subsurface irrigation and root zone water content measurement

In agricultural irrigation, the use of groundwater as a source of irrigation is minimal and given significantly less important because of its complexity, even though it may be a good alternative source of water to meet the irrigation demand (Cordeiro et al. 2016).

Understanding crop water uptake patterns and soil water flow within the root zone is critical for designing effective irrigation and drainage systems. Plant water uptake significantly impacts water and nutrient redistribution throughout the root zone of crops. As a result, understanding the water uptake pattern requires knowledge of root dispersion (Satchithanantham et al. 2014). Plants' extraction of soil water has been characterized at various degrees of complexity to determine the rate of water uptake from the soil as driven by the atmospheric conditions (Stalham and Allen 2004).

Stalham and Allen (2004) mentioned that it is evident that precise assessments of current water intake and rooting depths are critical for evaluating the crop's water needs. Because these will fluctuate during the season and be impacted by soil conditions in each field (or portion of a field), advances in water usage efficiency will necessitate a much deeper understanding of the importance of root development. Improved scheduling has both practical and environmental benefits.

Satchithanantham et al. (2014) suggest that subsurface drainage is used in agriculture to manage the groundwater table beneath the root zone of the crop and remove extra soil water to prevent water logging.

Kaja (2017) also added that excessive water restricts the root zone's ability to breathe during the crop-growing season. Subsurface drainage can be employed to remove excess water. Using drainage control structures regulates the drain output and preserves a shallower water table.

This study focuses on the root water uptake pattern for the canola plant at the final stage of the season to enable us to understand better the soil water dynamics within a fully developed root zone.

3.0 Materials & Methods

3.1 Laboratory study

3.1.1 Soil sample preparation

The efficiency of the sensors was assessed in three soils with different soil textures. The soil samples were clay soils from Arborg, Manitoba, sandy loam from Hespler Farms, Winkler, Manitoba, and sandy soil purchased as Play-sand. Soil samples consisting of different target moisture content of the three different soil textures were prepared. The different target volumetric water contents (VWC) were: 10, 20, 30, 40, and 50%. The target water contents were attained according to the bulk density and porosity of the soil. The prepared samples were placed in plastic containers, as shown in Fig.3.1.

Fig. 3.1 Prepared sand soil samples

The Volumetric Water Content (VWC) of the soil was calculated using the dry bulk density, dry and wet mass of the soil. The dry bulk density (ρ_b) of the sample was calculated using the given Eq. 3.1

$$\rho_b = \frac{m_s}{V} \tag{3.1}$$

Where:

m_s = mass of the soil (g),

V = total volume of the soil (cm^3).

Five containers of three different soil textures each were prepared to create soils with different target VWC. Steps on the preparation of soil samples with an appropriate target range of moisture content involve the following steps.

(1) Soil samples were dried in the oven for 24 hours to release the moisture in them and reach the residual moisture content (varies with soil texture types).

(2) The water of known volume was poured into each container and the level was marked.

(3) Soil samples were filled to the marked volume and weighed to get the mass of the dry soil.

(4) The bulk density of each soil sample was calculated using the volume and mass obtained in Steps 2 and 3, respectively.

(5) The porosity of the sample was calculated using the following equation 3.2

$$\text{porosity } (\varphi) = \frac{\rho_b}{\rho_s} \quad (3.2)$$

where:

ρ_b = dry bulk density

ρ_s = particle density obtained from the literature (Radcliffe and Simunek 2010)

(6) Using the porosity of the soil sample, the required amount of water was added to the sample to attain the target VWC of 10, 20, 30, 40, and 50%, and the soil was mixed well with a spatula without losing the soil.

(7) The wetted soil samples were covered with plastic film to prevent evaporation and kept for 72 hours to equilibrate to get even moisture content.

The soil samples of different VWCs prepared as above were used to calibrate the soil moisture sensors. All the above procedures were repeated three times for a total of 39 (twelve sand samples, fifteen loam samples, twelve clay samples) soil samples.

Most soil particles have a constant density of 2.65 g cm^{-3}, or around the density of quartz. Due to the stability of the value, the measurement is not frequently performed. While samples with high levels of organic matter have lower particle densities, samples with high levels of iron have slightly greater particle densities.

3.1.2 Capacitance soil moisture sensor (SEN0193)

The capacitance soil moisture sensor (SEN0193) (DF Robot, Shanghai, China) is one of the commercially available low-cost sensors, which works based on the capacitance principle. Based on the dielectric properties of the water, air, and soil mixture, the sensor transmits a voltage

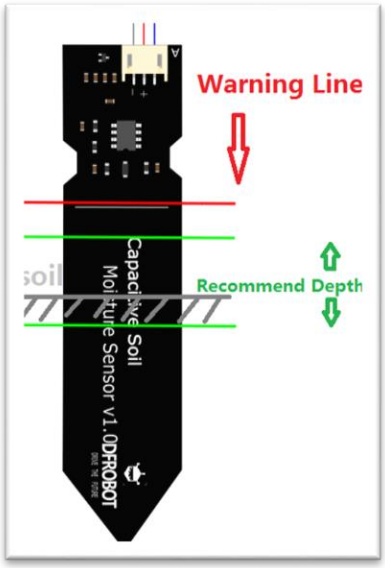

Fig. 3.2 Capacitance Soil Moisture sensor v1.0

output. As in fig. 3.2 shown below this sensor has two major parts. The top portion of the sensor contains the electronic circuits. The bottom portion includes the sensing. The optimum operating.

the voltage range is 3.3 V ~ 5 V (DF Robot 2015). This sensor has a built-in voltage regulator. These voltage regulators can be amplified using an Analog Digital Converter (ADC). This sensor is made of corrosive-resistant material.

Using the pulse generator, the SEN0193 sensor integrates the current as the charge accumulates for a fixed time by applying the repeating step voltage to the electrodes. Following that, the RC filter detects the current charge and discharge for that fixed time in the capacitor and produces the triangular waveform. The attached peak detector detects the peak of the triangular waveform and delivers the analog output. This output of voltage is related to the relative permittivity which is proportional to the water content.

Prevent short-circuiting the electronics, the manufacturer recommended inserting the sensor up to the line drawn in the sensor as shown in Fig. (3.2). However, the electronics were encased in beeswax to protect them from getting wet and allow us to embed the probe into the soil.

3.1.3 TEROS 10 (T10)

Teros 10 (T10) (Meter Environment, Washington, USA) capacitance-based soil moisture sensors are one of the commercially available sensors, designed to monitor the moisture content

Fig. 3.3 TEROS 10 (Meter Environment)

of the soil. The T10 sensors measure the VWC and store it in the cloud using the data logger designed by the Meter group. The T10 sensor measures with an accuracy of 0.03 m3/m3 in soil media in a volume of influence of 430 mL as per the manufacturer's instruction (M. Environ. 2018).

Since the T10 sensor has its own factory-developed calibrations, it can be taken to the field directly to measure soil moisture content. It can withstand all weather conditions and can be left in the field for over 10 years to collect the SWC data. As in fig. 3.3 shown below T10 sensors two major parts like SEN0193 sensors.

(1) Sharp-edged stainless-steel sensing needles.

(2) The electrical circuit part is enclosed and protected.

3.1.4 Sensor preparation

Capacitance soil moisture sensors (SEN0193) need the electrical circuit part protected from water. In this study, sensors were buried entirely in the soil at a depth of 20 cm and 40 cm. Beeswax was used to protect the electronic circuits in the sensor. Sensor wires were stripped, and a 1-meter extension wire was attached. Polyvinyl Chloride (PVC) pipes were used to enclose the wires to protect them from the field rodents. A one-inch slot was made at the end of the pipe to hold the sensor. Beeswax heated up to 200^0C and poured in between the sensor and the PVC pipe junction. T10 Sensors were used as it is for the lab study.

3.1.5 Internet of Things (IoT) Devices

3.1.5.1 Raspberry Pi b3+

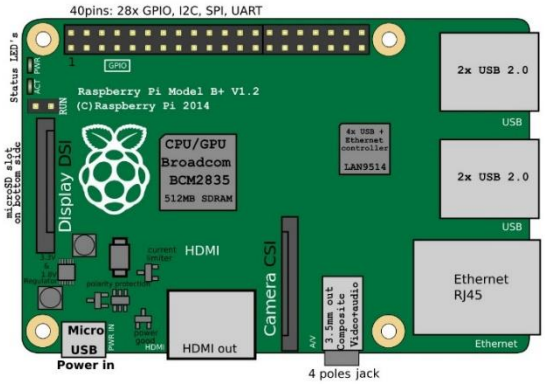

Fig. 3.4 Raspberry Pi B3+

Raspberry Pi (Fig.3.4) is a minicomputer used to control sensing devices and weather monitoring devices because it is low-cost, open-design and easy-adaptability. It employs a system on a chip, which combines the CPU and GPU into a single integrated circuit, with the RAM, USB ports, and other components soldered to the board for an all-in-one solution. For IoT devices, the Raspberry Pi may function as an “Internet Gateway”. The Raspberry Pi functions as a web server for uploading and transmitting sensor data to the cloud. SEN0193 sensors can be monitored through Raspberry Pi to store the VWC data and upload the data to the cloud system.

3.1.5.2 Arduino Uno

The open-source programmable microcontroller board Arduino UNO (Fig. 3.5) is a low-cost, adaptable, and user-friendly device that may be utilized in a variety of electrical applications. With the ability to interact with other Arduino boards, Arduino shields, and Raspberry Pi boards, this board has an output that can control sensors, relays, LEDs, servos, and motors. The SEN0193 sensors were created to function with Arduino. We may create programs (C++ with additional functions) using the Arduino IDE software that helps control the sensor devices. It can be easily integrated with Raspberry Pi b3+, In this study, Raspberry Pi b3+ was used to monitor the Arduino, which collects the VWC data.

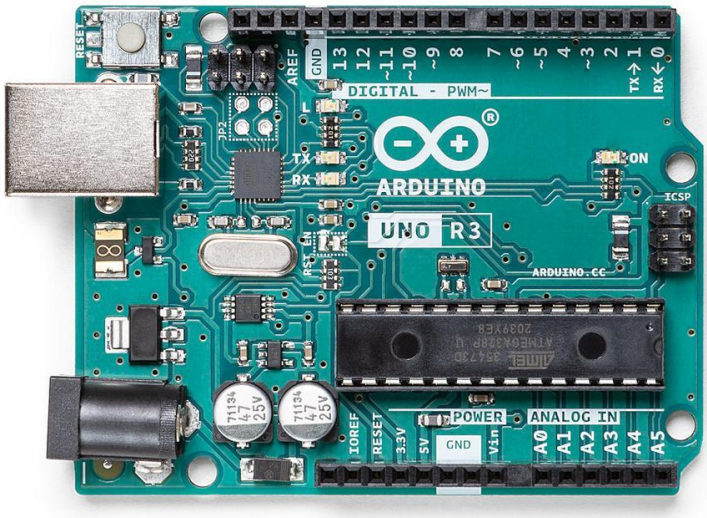

Fig. 3.5 Arduino Uno

3.1.5.3 ADS1115 Analog to Digital Converter (ADC)

The ADS1115 (Fig. 3.6) is a 16-bit precision ADC with four multiplexed inputs that may be used singly or in pairs for differential measurements. It features a calibrated reference that can detect negative voltage built in for extreme precision. The built-in programmable gain amplifier can amplify small signals up to sixteen times. Noise cancellation is also included on the board to

keep the supply lines clean. Arduino can connect to only one sensor, which is a limitation of this study. ADS1115 allowed us to connect multiple SEN0193 sensors to a single Arduino. The main use of ADS115 was to broaden the data range from a narrow range (200-500) to a wider range (9000-20000). In this case, even small changes in VWC can be identified. So, ADS1115 was needed for this study. Using the following Arduino program, the sensors were logged.

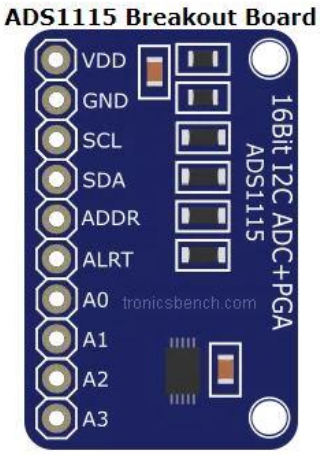

Fig. 3.6 ADS1115 Analog to Digital Converter

```
#include <Wire.h>

#include <Adafruit_ADS1015.h>

Adafruit_ADS1115 ads1115(0x49);   //For DFRobot

Adafruit_ADS1115 ads(0x48);  //For meter

void setup()

{

  Serial.begin(9600);
```

```
  //put your setup code here, to run once:
  ads1115.setGain(GAIN_ONE);
  ads1115.begin();
  ads.setGain(GAIN_ONE);
  ads.begin();
}
void loop()
{
  // put your main code here, to run repeatedly:
  int16_t adc00, adc01, adc02,adc10,adc11,adc12;
  adc00 = ads1115.readADC_SingleEnded(0);
  adc01 = ads1115.readADC_SingleEnded(1);
  adc02 = ads1115.readADC_SingleEnded(2);
 // adc10 = ads.readADC_SingleEnded(0);
  Serial.print(adc00);
  Serial.print(",");
  Serial.print(adc01);
  Serial.print(",");
```

```
  Serial.print(adc02);
  Serial.print(",");
  Serial.print(adc10);
  Serial.println("");
  delay(1000);
}
```

3.1.6 Integration of Raspberry Pi and Arduino with the sensor

Five capacitance soil moisture sensors (SEN0193) were used in the laboratory study to get the calibration equation. Using the ADC, we could connect to fourteen sensors using the two different address ports in the ADC. Each sensor has three connecting points such as (1) input, (2) Output, and (3) data collection. Jumper wires were used to connect the ADC and Arduino via a breadboard. Arduino is a software-based open-source microcontroller, which helps monitor or control sensors, GPS units, the internet, smartphones, etc., SEN0193 sensors with the ADC were connected to the microcontroller. Arduino programming codes were written in the IDE (Integrated Development Environment) software that was used to collect the data from the sensors. Arduino IDE software is compatible with UNIX and Windows Operating Systems. The Arduino and sensors circuit can be used to collect the data at fixed time intervals but cannot store or transfer the data. The Raspberry Pi B 3+, a minicomputer was integrated with the system using the python programming language to store the data on a memory card.

The code was written to collect the data from the sensors at fixed time intervals. The sensor number, date, time, and voltage readings were stored as a .csv file.

```
import serial
import time
import csv


import io
from google.cloud import storage
import datetime
import firebase_admin
from firebase_admin import credentials, firestore
import os


PROJECT_ID = 'authdemo1-ee4e4'
CLOUD_STORAGE_BUCKET = 'authdemo1-ee4e4.appspot.com'

filename = 'RPiGSM1.csv'

credential_path = "/home/pi/Desktop/authdemo1-ee4e4-firebase-adminsdk-8hp9r-4cbdc9d3cc.json"
os.environ['GOOGLE_APPLICATION_CREDENTIALS']=credential_path
cred = credentials.Certificate("/home/pi/Desktop/authdemo1-ee4e4-firebase-adminsdk-8hp9r-4cbdc9d3cc.json")
firebase_admin.initialize_app(cred)

ser = serial.Serial('/dev/ttyACM0') #This must match the port shown on the Arduino IDE program
ser.flushInput()
```

```
client = storage.Client(project=PROJECT_ID)
        # Instantiate a bucket
bucket = client.bucket(CLOUD_STORAGE_BUCKET)
        # Instantiate a blob
blob = bucket.blob(filename)



# The public URL for this blob
url = blob.public_url

while True:
    try:
      ser_bytes = ser.readline()
      new = ser_bytes.split(",")
      count = len(new)
      try:
        print time.ctime(int(time.time()))
        for i in range(count):
          print "sensor %d reads" %i, new[i]
      except:
        continue
      with open("/home/pi/DFrobot1.csv","a") as f:
        writer = csv.writer(f,delimiter=",")
        # #writer.writerow(["","Sensor 0","Sensor 1","Sensor 2"])
        writer.writerow([time.ctime(int(time.time())),new[0],new[1],new[2]])
```

```
    with open("/home/pi/DFrobot1.csv", "rb") as fp:    # Upload the file
      blob.upload_from_file(fp)
  except:
    continue
```

Access data remotely, Raspberry Pi needs to be added with a Wi-Fi module, which transforms a serial port or TTL level (transistor-transistor logic) into an embedded module that can comply with Wi-Fi wireless network communication standards using a built-in wireless module. A SIM card module was used to transmit the data to the cloud.

3.1.7 Data Collection

Two sets of laboratory experiments were conducted to get the calibration equation and for the validation.

(1) SEN0193 sensors with three major types of soils to get the calibration equations.

(2) Both SEN0193 sensors and T 10 Sensors were tested with the same set of soils for validation.

Five SEN0193 sensors were embedded into the soil ensuring there is no air gap between the sensor and the soil around the sensor as shown in fig. 3.7. The Raspberry Pi integrated system was connected to collect the data in 10-minute time intervals for an hour. Soils from the experimental sites were prepared with target VWC using appropriate volumes of water as used in the lab study. Based on this lab study, calibration equations were developed for each type of soil. The Gravimetric Water Content of the soil samples was measured using the gravimetric method and converted into VWC using laboratory-measured Bulk Density (BD).

Fig. 3.7 Laboratory data collection with SEN0193 sensors.

For validation, the T10 Sensors were used as another comparison method. Three T10 sensors were used against three SEN0193 sensors in the three different soils with three replications and five different soil water content levels as in fig. 3.8. The T10 sensors ran with factory developed software program called Zentra cloud software with ZL6 data logger for the time interval of 10 minutes for an hour. Validation curves were developed using the data collected from both SEN0193 sensors and T10 Sensors.

Fig. 3.8 Laboratory data collection with SEN0193 sensors and T10 Sensors.

3.2 Field study

Two sets of field experiments were conducted to get the root zone VWC and for validation.

(1) SEN0193 sensors were buried at 20 cm and 40 cm in clayey lacustrine soil

(2) SEN0193 sensors were buried in the Root zone area (0-100 cm) in the Winkler site (sandy loam lacustrine) in the canola crop.

3.2.1 SEN0193 sensors at 20cm and 40 cm depth

A field experiment was conducted in clay soil in Winnipeg. Six SEN0193 sensors were buried at 20 cm and 40 cm with two externally powered Raspberry Pi integrated systems as in fig. 3.10. All the 20 cm depth sensors were connected to one Raspberry Pi system as all the other 40 cm depth sensors.

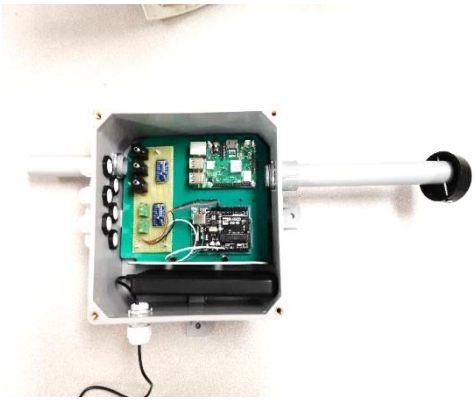

Fig. 3.9 Raspberry-Pi & Arduino integrated system

Data were collected continuously for two months with a time interval of 3 hours and stored. The stored data was accessed via Wi-Fi using a VNC viewer and remotely monitored for over 2 months. Soil samples were collected at different time intervals, where significant changes occurred. Boxes were made to keep the entire raspberry pi system in it to protect from harsh weather conditions, as shown in Fig. 3.9.

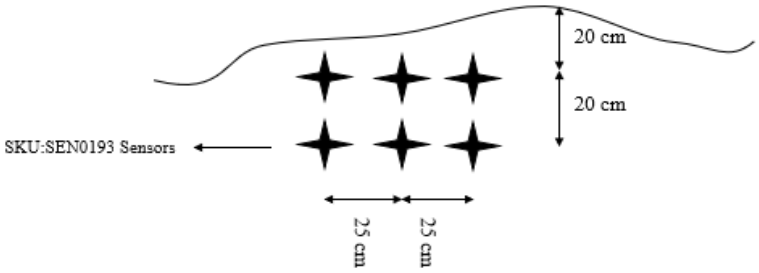

Fig. 3.10 SEN0193 Sensors at 20 and 40 cm depth

Validation curves were developed using the data collected to evaluate the accuracy of the sensors against the T 10 Sensor values and Actual VWC from the gravimetric method.

Fig. 3.11 Sensor arrangement at Winnipeg site

This study was conducted during the period from October 2021 to the end of November 2021. The site had a pine tree with grass covering the soil. During the study period, the ground surface was covered with snow, as shown in Fig. 3.11. The temperature started to drop below 0 degrees Celsius by the end of October. The relative permittivity of water at 0^0C is 87.7 (Malmberg and Maryott 1956). Even though temperature affects the permittivity, in this study, the ground temperature at the site was not affected because the surface snow and the cover vegetation acted as a shield to retain the positive ground temperature at depth (Kahimba et al. 2008).

3.2.2 Root zone study on Winkler site

Canola root zone moisture content measurements were conducted by installing 12 SEN0193 sensors in the plant root zone area (0 cm – 100 cm) at four different depths (25 cm, 50 cm, 75 cm, 100 cm) on a space interval of 25 cm as in Figs. 3.13 and 3.15.

Fig. 3.12 Root zone water study on Winkler site

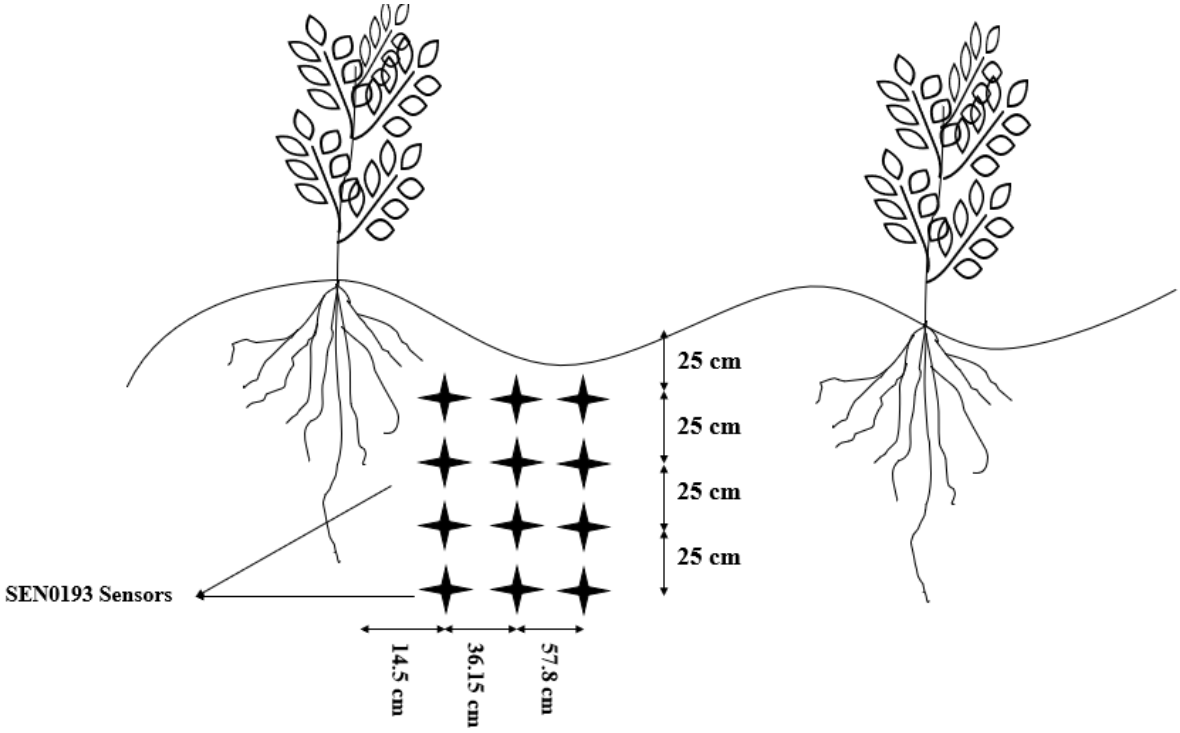

Fig. 3.13 Sensor arrangement on Winkler site

Sensors were buried at an angle of 60 degrees using an angular guide to prevent the preferential flow of water along the pipe, as shown in Figs. 3.12 and 3.14. To achieve equal

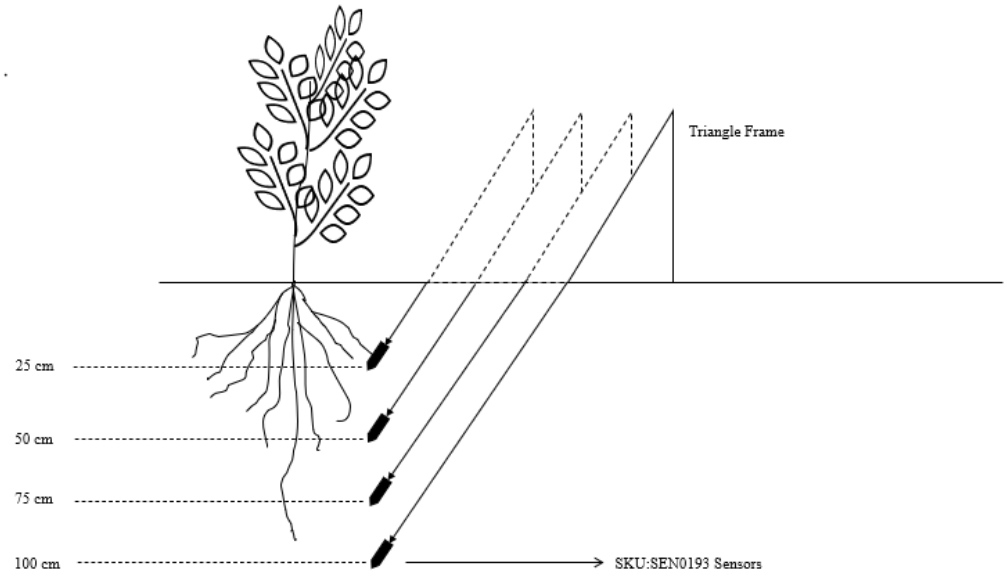

Fig. 3.14 Sensor arrangement around the root zone

spacing among the study plane of the root zone area, 25 cm depth probes were moved 14.5 cm away from the plant base and embedded at the depth of 28.9 cm (Fig. 3.13). All the 50 cm depth probes were moved 28.9 cm away from the plant base and embedded at a depth of 57.8 cm. Probes for 75cm depth were placed at 43.4 and a depth of 86.6 cm. To reach 100 cm with a 60-degree angle, probes were inserted 57.8 cm away from the plant and buried at a length of 115.5 cm. The research was conducted towards the end of the cropping season with well-developed roots.

Soil moisture data were collected continually at one-hour intervals over two months. The data was stored in an SD Card in the Raspberry Pi. Four raspberry-pi integrated systems related to twelve sensors (Figs. 3.14 & 3.15) and enclosed in a box to protect from the weather and field rodents. The soil texture type found in the Winkler site is known as "Gleyed Rego Black Chernozem" by the Canadian system of soil classification, which contains a surface texture of

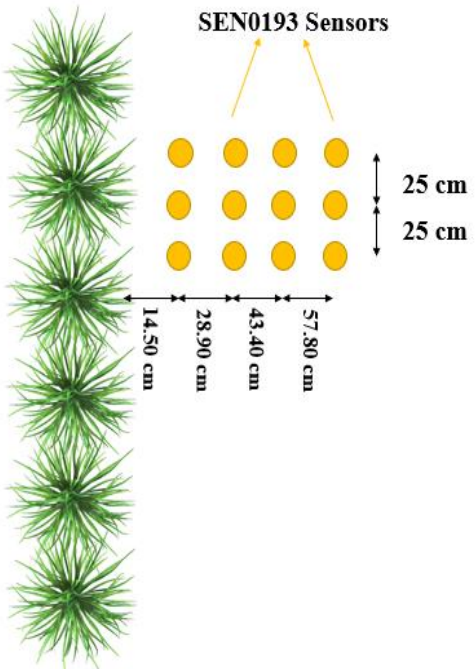

Fig. 3.15 Elevation of sensor arrangement at Winkler site

"fine sandy loam". During the installation on 13th August 2021, 16 litres of water were irrigated on the surface to study the water movement around the top layer of the soil (Fig. 3.12).

3.3. Statistical analysis of the performance of the calibration equations

The performance of the developed calibration equations was assessed both statistically and using validation figures. Plotting the predicted VWC values using the calibration equation against the observed VWC values to observe the fitness using the 1:1 validation line is a common way of evaluating the developed model. Statistical parameters (R^2, RMSE, MAE, MBE) to evaluate the performance of the water content studies were calculated.

3.3.1 Coefficient of determination (R^2)

When comparing measured and predicted values, the coefficient of determination (R^2) is employed to demonstrate the relationship. Its values vary from zero, which denotes complete disagreement, to 1, which denotes absolute agreement between observed and predicted values. Using the given Eq. 3.3

$$R^2 = \frac{\sum_{i=1}^{n}(O_i - \bar{O})\,(P_i - \bar{P})}{\sqrt{\sum_{i=1}^{n}(O_i - \bar{O})^2}\sqrt{\sum_{i=1}^{n}(P_i - \bar{P})^2}} \quad (3.3)$$

Where O_i are the observed VWC values, P_i are the predicted VWC values, $\bar{O}$ is the average of observed VWC values, $\bar{P}$ is the average of predicted VWC values and the n is the total number of observed VWC values.

3.3.2 Root Mean Square Error (RMSE)

The calculation of the mean difference between the observed and the predicted values is known as RMSE. It can be calculated by using equation 3.4

$$RMSE = \sqrt{\frac{\sum_{i=1}^{n}(O_i - P_i)^2}{n}} \quad (3.4)$$

3.3.3 Mean Bias Error (MBE)

The MBE provides the uniformity of error distribution as well as a measure of how well or poorly the model predicts the observed values. It can be calculated by Eq. 3.5

$$MBE = \frac{\sum_{i=1}^{n}(O_i - P_i)}{n} \quad (3.5)$$

3.3.4 Mean Absolute Error (MAE)

The weighted average magnitude of the absolute errors is measured by the mean absolute error (MAE) and calculated using equation 3.6.

$$MAE = \frac{\sum_{i=1}^{n}|O_i - P_i|}{n} \quad (3.6)$$

Well-developed model is attained when the R^2 is equal to 1, RMSE, MBE, and MAE are equal to 0 (Mkhabela and Bullock 2012).

4.0. Results and Discussion

4.1. Bulk density (ρ_b), Porosity(Ø), and Volumetric water content (θv)

The bulk density of the soil decreases if the soil porosity increases. Sandy soils have a higher bulk density than loam or clay soils because their total pore space is less. Typically, bulk densities fall between 1.1 and 1.8 Mg m^{-3}. It is affected by soil organic content, texture, mineral density, and packing arrangement. The porosity values of the soil samples are shown in Fig. 4.1.

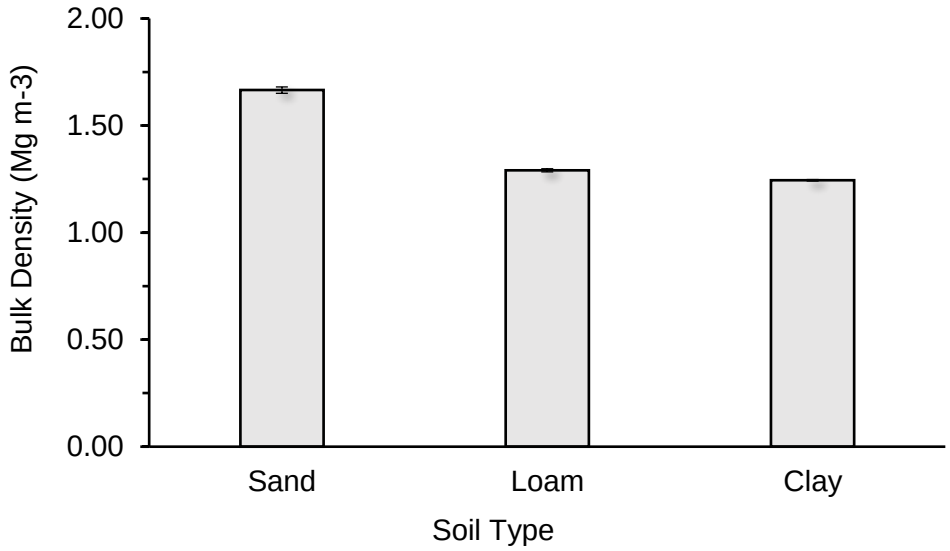

Fig. 4.1 Bulk density of the laboratory soil samples.

As in fig. 4.1 bulk density of the laboratory-prepared sandy soil samples was 1.66 Mg m^{-3}, which is a slightly higher value for sandy soils. The standard error for the sand sample found during the laboratory calculation was 0.014 Mg m^{-3}. The method of packing the soil column affects the soil bulk density and tapping or pressure on the surface affects the packing. Samples that are disturbed during the study might lead to a higher bulk density.

The bulk density of the loam sample was 1.29 Mg m^{-3}, which is a much lesser density compared to the average loam soil bulk density. The loam samples used in this study were a

mixture of loam and clay components since it was collected from the agricultural field. Due to the presence of fine particles in the sample, the bulk density of loam was quite close to the lowest bulk density range. the standard error for the loam sample's bulk density was 0.007 Mg m^{-3}.

Clay soil samples had a bulk density of 1.24 Mg m^{-3} with a standard error value of 0.003 Mg m^{-3}. The clay sample bulk density was within the average range of bulk density for clays.

Porosity varies with the soil texture, structure, and location where the sample is collected. The pore space, which is either filled with air or water, between mineral particles (and solid organic matter) in the soil is known as porosity. During the laboratory calculation, the porosity of the soil samples was found to vary from 36 to 52 percent.

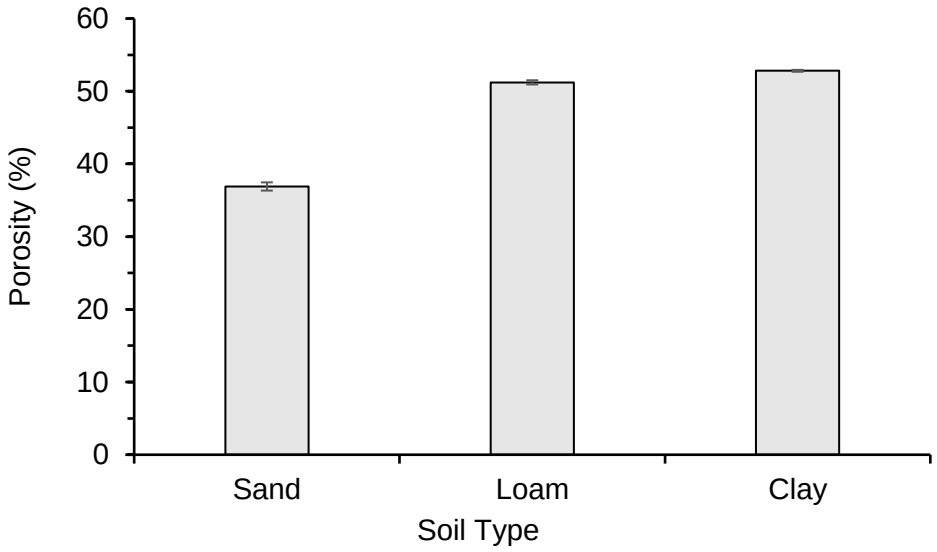

Fig. 4.2 Porosity of the laboratory soil samples.

As in Fig.4.2 standard error of porosity in the sand sample was 0.56% with a porosity of 36%. Sandy soil contains much higher coarse particles compare to the loam and clay textural type soils. A diameter range of 0.05 to 2 mm soil particles are considered as coarse sand.

Loam soil samples were found to have a porosity of 51.2 % and the standard error was found to be 0.29%. Loam soil particle sizes (diameter) are in the range of 0.02 to 0.002 mm. The clay sample porosity did not deviate much from the loam sample. The highest porosity of 52.8 percent was found in the clay samples with a standard error of 0.13%. Soil particle diameter, which is found to be less than 0.002 mm categorized as clay.

Soil samples were mixed with a calculated amount of water based on their respective porosity to attain the desired volumetric water content. Volumetric water content (θ_v) was calculated using the bulk density and gravimetric water content (θ_g). The actual VWC

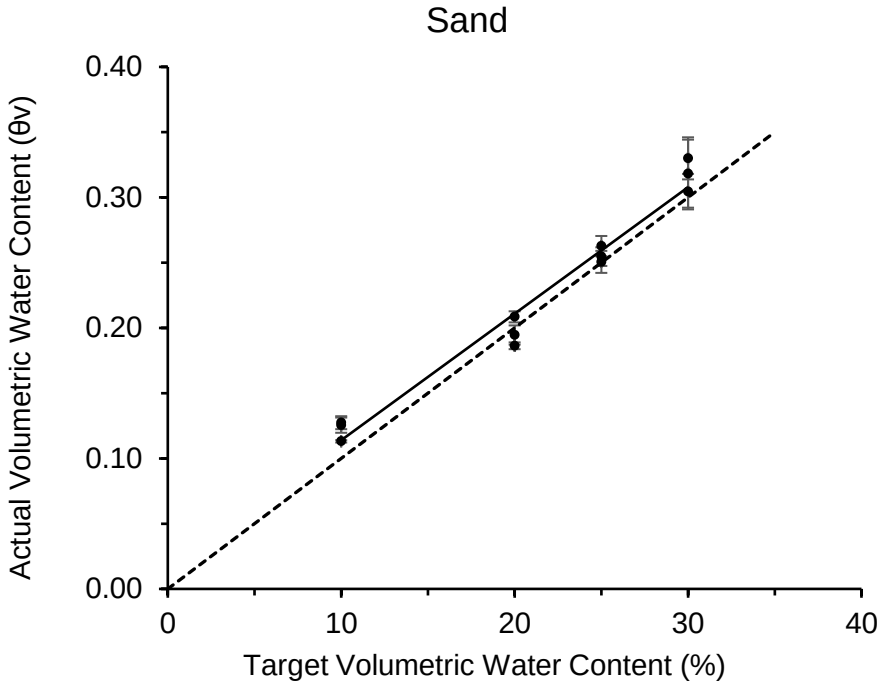

Fig. 4.3 Volumetric wate content of the sand samples.

was plotted against the target VWC as shown in Fig.4.3. Due to the destructive nature of the sample preparation and evaporation, replicates produced were not found in the same water content as expected. For example, the three 10% target sand sample's water content (θ_v) was found 0.125 ±

0.005, 0.113 ± 0.001, and 0.127 ± 0.004 m^3/m^3 for respective samples (Fig. 4.4). Same phenomena occurred for all the soil samples.

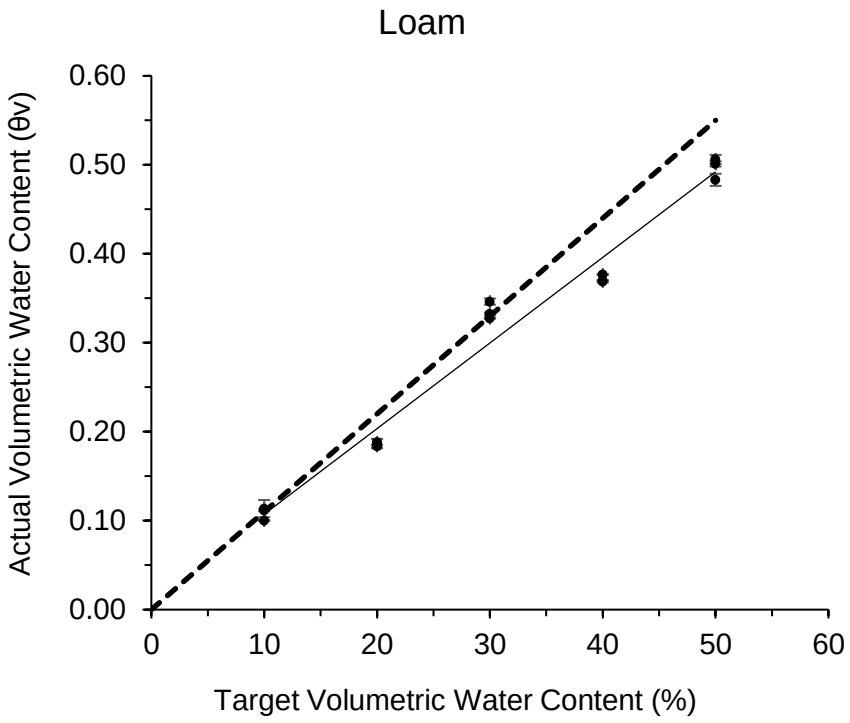

Fig. 4.4 Volumetric water content of the loam samples.

As in Fig. 4.4, Loam samples were found to have higher water content than clay soil samples (Fig. 4.5). Loam soil samples used in the study were from the Hespler Farms, Winkler, Manitoba, which contains higher fine particles (fine sandy loam). Due to the fine structure of the soil, samples retained the water content (θ_v) of 0.050 ± 0.005 m^3/m^3. The 40% target samples were found to have less water content (θ_v) of 0.36 ± 0.001, 0.37 ± 0.0003, 0.36 ± 0.0003 m^3/m^3 due to denser packing during mixing.

Clay soil samples used in the study were from the PESAI (Prairies East Sustainable Agriculture Initiative) site (Arborg, Manitoba, Canada) and categorized under the texture type of heavy clay. High clay content leads to the expansion and contraction of the soil according to the amount of water present in it (Ndulue and Sri Ranjan, 2022).

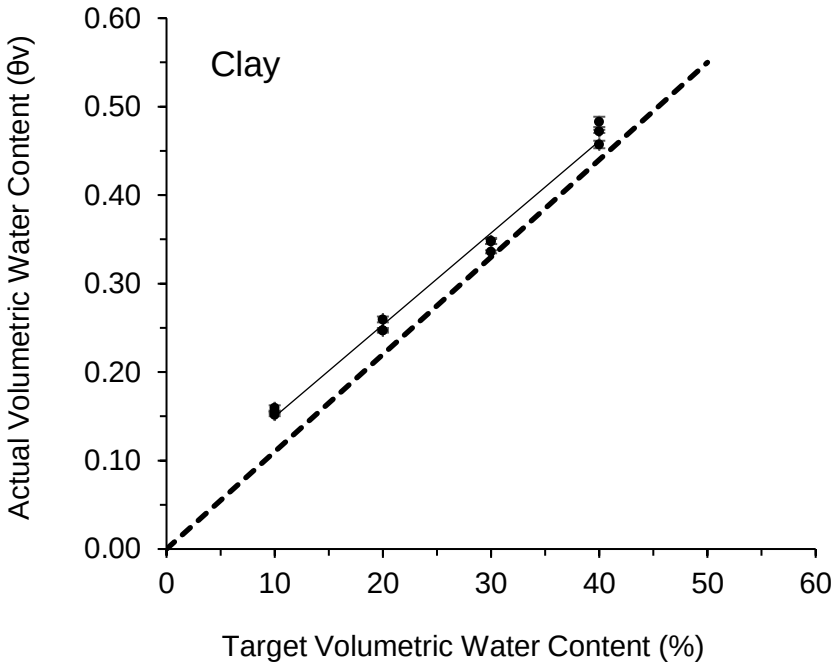

Fig. 4.5 Volumetric water content of the clay samples.

The presence of heavy clay soil particles in the samples retained the higher water content (θ_v) of 0.49 ± 0.005 m^3/m^3 (Fig. 4.5). The VWC of the clay samples was found to be almost distributed evenly for the moisture percentage of 15, 25, 35, and 45 with small variation between the replicates. In all the sand and clay samples, the VWC was found to be slightly higher than the target VWC (Figs. 4.3, 4.4, & 4.5). Compared to the sand and clay samples, the VWC of the loam followed a different trend. For the target VWC of 20% and 50%, the loam sample VWC was on the lower side, but 30% and 40% target VWC samples were on the higher side. The target VWC of 10 percent of samples remained around the same VWC as expected (Fig. 4.4).

4.2. Correlations of sensor reading to VWC during the lab experiment

Correlation graphs were plotted individually for all three soil texture types to get the best-fitting equation. Third-order polynomial equation from the plotted graph was used as a calibration equation with the highest regression value (Figs. 4.6, 4.7, and 4.9). The SEN0193 sensors worked very well with a correlation of 91% in sand, loam, and clay.

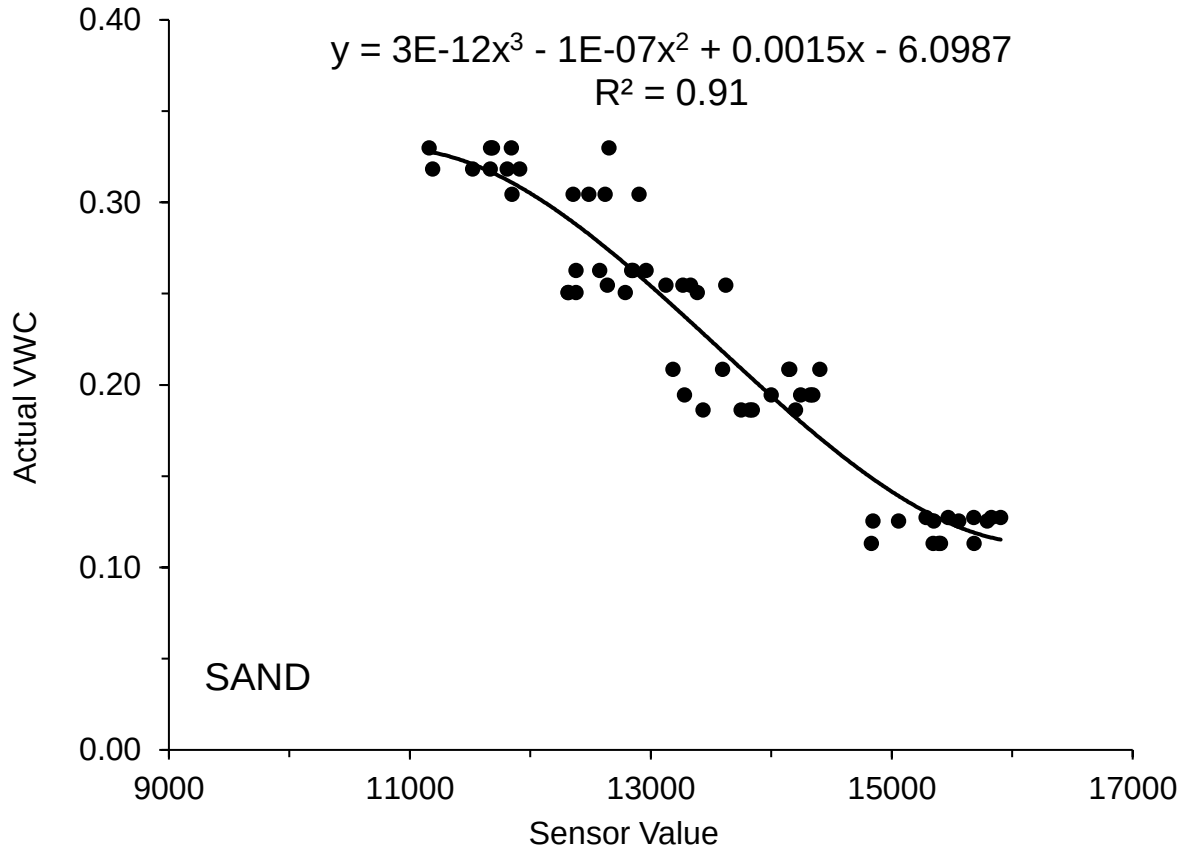

Fig. 4.6 Correlation of the SEN0193 values with actual VWC in sand.

Five different SEN0193 sensors were used to measure 12 different VWC sand samples. As shown in Fig 4.6, each SEN0193 sensor gave a range of values for each of the VWC present in the soil sample. For VWC 0.113 ± 0.001 m^3/m^3, sensor value ranged from 144800 to 15700, Which proves that individual SEN0193 sensor produces different range of sensor value for the same VWC

(Fig. 4.6). Similarly, VWCs of 0.30 ± 0.01, 0.25 ± 0.008, and 0.20 ± 0.004 m3/m3 sensor values were found in the range of 12900 to 13200. Even though the correlation between the sensor value and VWC was 91% for the calibration equation, the possibility of predicting the VWC with accuracy might be affected by the different behaviour of individual sensors.

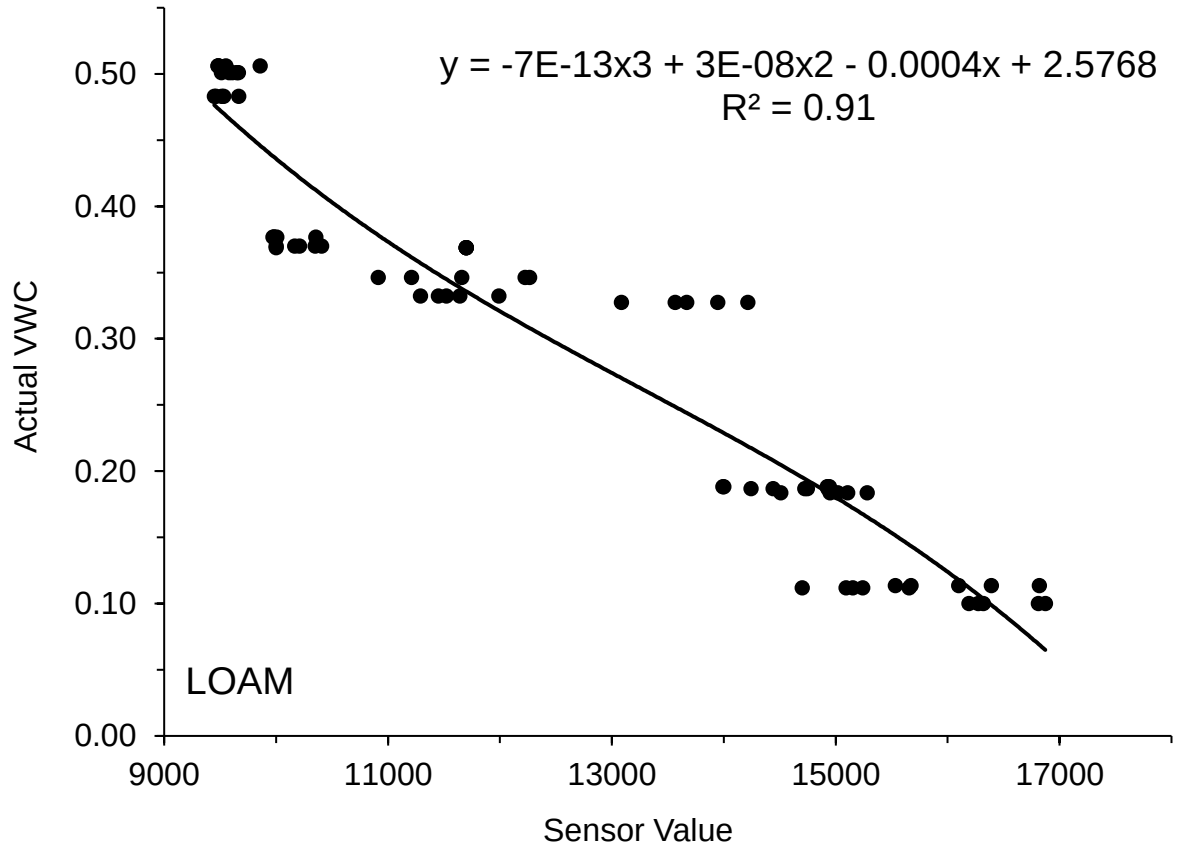

Fig. 4.7 Correlation of SEN0193 sensor value with actual VWC in loam

The loam calibration was carried out using 15 different VWC samples with 5 SEN0193 sensors to develop the calibration equation as shown in Fig. 4.7. The range of sensor value variation was found to be higher in loam samples than in sand and clay. For VWC of 0.33 ± 0.001 m^3/m^3 and 0.32 ± 0.0004 m^3/m^3 sensor values varied from 11200 to 14200 (Fig. 4.7). At 50% target VWC, the range of the sensor values was narrower. During the study, loam, and clay samples after reaching the equilibration stage at room temperature, moisture on the surface of the samples started

to evaporate. At that point, the mixture gets cracks on the top layer, creating an air gap as in Fig. 4.8. A wide range of variation in the sensor values was recorded due to the air gap created between the sensor and the soil surface. The ratio between the dielectric constant of air and water is 1:80 (Topp et al. 1980b). Since SEN0193 sensors depend on the media's dielectric property and the sensor's exposure to the air affects the performance.

Fig. 4.8 Cracks on the soil sample.

For better performance of the sensors, no air gaps should be present. The laboratory measurements were done in a controlled environment. During the study, the room temperature was set to 22^0C because Radi et al., (2018) mentioned that temperature change had a slight impact on the performance of the sensor.

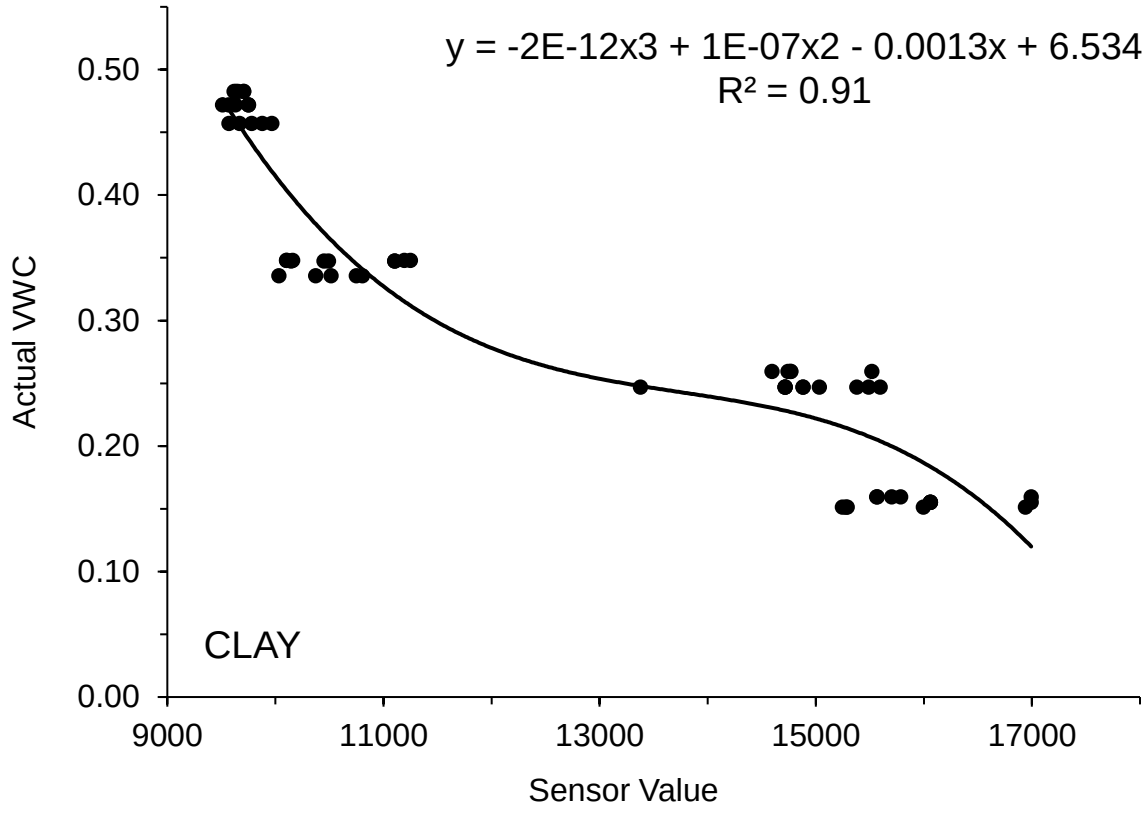

Fig. 4.9 Correlation of SEN0193 sensor value with actual VWC in clay

Clay samples with 12 different VWCs were used to evaluate the performance of five SEN0193 sensors. (Ndulue and Sri Ranjan, 2022), The clay soil samples were found to develop surface cracks over time (Fig. 4.8). As shown in Fig. 4.9, compared to the loam calibration, the variation of sensor values was found to be lesser in clay samples. However, for the 20% target sample with an actual VWC of 0.25 ± 0.001 m^3/m^3 the variation range was found to be wider (13300 to 15600) than other samples (Fig. 4.9). Due to the surface cracks, the sensor's performance in the clay sample was affected by the air gap created between the sensor and the soil.

4.3 Calibration model performance

Calculated statistical parameters for the developed calibration model were shown in Table 4.1. Validation visual plots showed the accuracy of the developed calibration equations. The overall performance of the calibration was evaluated by the R^2, RMSE, MAE, and MBE.

Table 4.1 Summary of statistical parameters for calibration equations.

	Acceptable range	Sand	Loam	Clay
R^2	closer to 1	0.902	0.907	0.870
RMSE(m^3/m^3)	closer to 0	0.02200	0.04328	0.03506
MBE (m^3/m^3)	closer to 0	-4.05E-15	-1.95E-16	5.92E-15
MAE (m^3/m^3)	closer to 0	0.01760	0.03370	0.03123

Statistical indices of sand calibration show that RMSE (0.02200 m^3/m^3) and MAE (0.01760 m^3/m^3) were closer to zero (Table 4.1), which indicates the satisfactory performance of developed sand calibration equations. Negative MBE (-4.05E-15 m^3/m^3) indicates the underprediction of the equation and R^2 (0.902) was closer to one.

The loam calibration equation showed a good performance with RMSE and MAE of 0.04328 m^3/m^3 and 0.03370 m^3/m^3 respectively (Table 4.1). The loam equation underpredicted the VWC values based on the negative MBE of -1.95E-16 m^3/m^3 with R^2 of 0.907.

R^2 (0.870) of clay calibration was found to be lesser than the sand and loam. Clay calibration showed the overprediction of VWC values with a positive MBE of 5.92E-15. RMSE and MAE of clay calibration were found to be 0.03506 and 0.03123, which resided closer to zero. A satisfactory model is obtained when the RMSE, MAE, and MBE are equal to 0 and R^2 is equal to one (Mkhabela and Bullock 2012). All three developed equations RMSE, MAE, MBE, and R^2 resided within the acceptable range.

4.4 Validation under laboratory conditions.

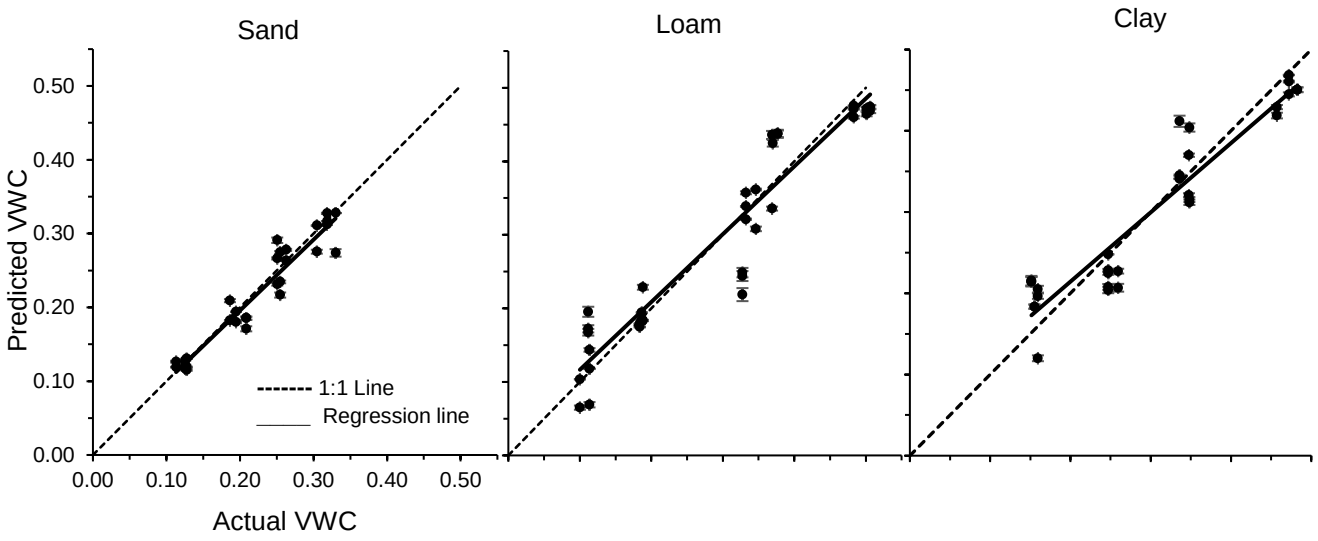

Fig. 4.12 Validation of sand calibration **Fig. 4.11 Validation of loam calibration** **Fig. 4.10 Validation of clay calibration**

A subset of data obtained at different target VWCs was plotted against the predicted VWC obtained by inputting the sensor data into the calibration equations obtained for the different soil types (Figs. 4.10, 4.11, & 4.12). The wide range of variation in sensor values in loam and clay samples affected the performance of the respective calibration equations. However, the higher R^2 value and the closeness to the target 1:1 line show that most of the predicted VWC were either under-predicted or over-predicted for all three types of soils as shown in Figs. 4.10, 4.11, and 4.12.

The average standard error on the prediction of VWC for sand was found to be 0.002 m^3/m^3 (Fig. 4.10). The regression lines were plotted to evaluate the equation's accuracy (solid line in Figs. 4.10, 4.11, & 4.12). Small error bars indicate that the precision of the developed calibration equations is good. The regression line closely follows the 1:1 line till the 15% target VWC and beyond this, it is over or under-predicted (Fig. 4.10). Use of third order polynomial equation is prone to underpredict the VWC values (Rowlandson et al. 2013).

The loam calibration equation mostly overpredicted the VWC values till 25% of the target VWC, and the regression line was found to deviate from the 1:1 line by 2% around the lower VWC values (Fig. 4.11). Most of the VWC values were underestimated for the range of 25 % to 50 %. Compared to the sand, the loam equation resulted in lower accuracy at the actual VWC of 0.33 m^3/m^3 and 0.11 m^3/m^3. The accuracy of predicting the actual VWC from the calibration equation was affected by the wide range of variation in sensor values.

The regression line for the clay calibration equation also followed the same trend as the loam equation, as shown in Fig. 4.12, with a deviation of 4% from the 1:1 line at 0.15 and 0.48 VWC values. The mean standard error calculated for the predicted VWC values was 0.003 $m^3/m^{3,}$ which was comparatively higher than that for sand and loam. Based on the texture type of the soil (heavy clay) with higher fine particles, the errors associated with predicting the VWC were found to be higher. This finding is supported by several studies (Topp et al. 1980a; Yu et al. 1997; Rowlandson et al. 2013).

Clay soils tend to have a higher specific surface area by nature. In this case, the dielectric constant would be lower. The SEN0193 sensor depends on the dielectric constant of the matrix being used to measure the values. Therefore the VWC would be underpredicted, affecting the accuracy of the equation (Roth et al. 1990). At the actual VWC of 0.26 m^3/m^3 the underpredicted VWC values were 0.21 ± 0.005 m^3/m^3 and 0.23 ± 0.003 m^3/m^3 (Fig. 4.12).

4.5 Validation of equations in the Winnipeg experiment site.

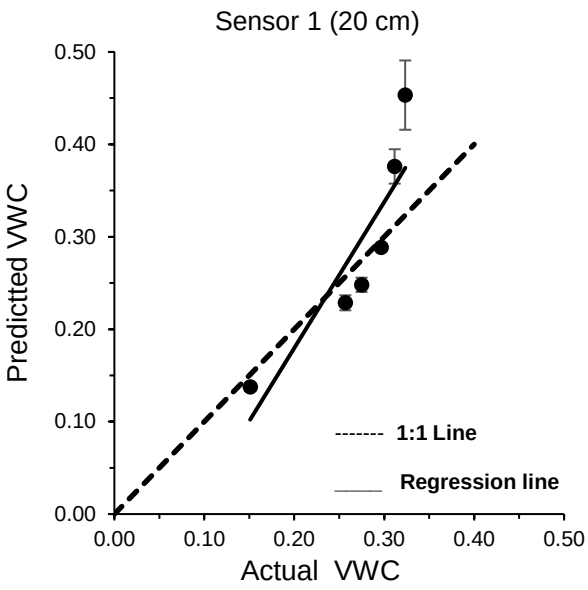

Fig. 4.13 Field validation of sensor_1

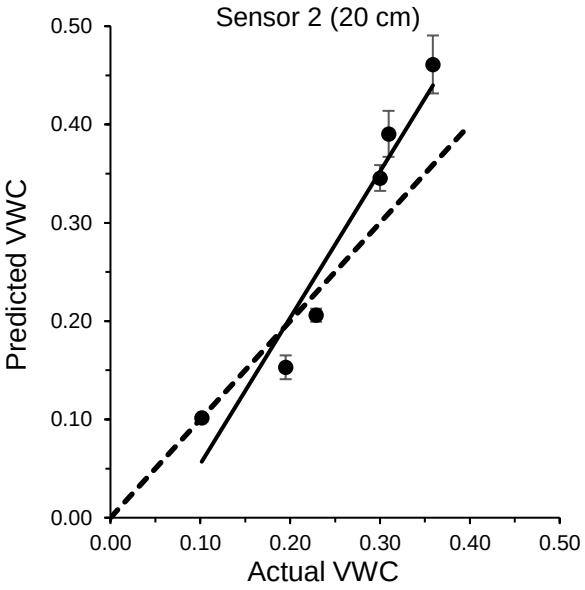

Fig. 4.15 Field validation of sensor_2

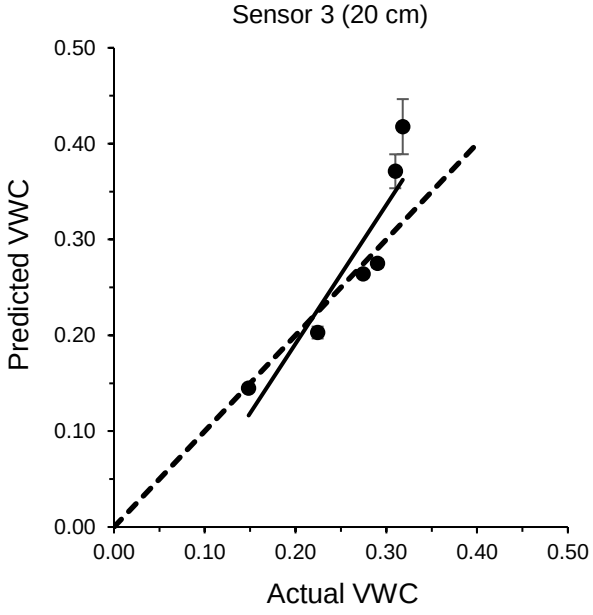

Fig. 4.14 Field validation of sensor_3

Field validation of the developed calibration equations was carried out in loam. The predicted VWC values were calculated using the loam calibration equation and plotted against the VWC values of the soil samples collected at the experimental site. The actual VWC values were measured in the laboratory using the gravimetric method (Figs. 4.13, 4.14, 4.15, 4.16, 4.17, & 4.18). During the study, the top surface was covered by snow and with little vegetation cover. The evapotranspiration (ET) rate was much lower than normal field conditions. The performance of each of the six sensors was evaluated using the validation plots. The average temperature recorded during the study period was 3.2 to -2.0 degree Celsius (Weather Canada).

All three sensors, at 20 cm depth, followed the trend of overestimating the VWC when the water content of the soil was high. The standard error for the overpredicted VWC was also found to be larger at a higher soil water content. The standard errors on predicting the VWC by sensor_1, sensor_2, and sensor_3 was found to be 0.013 m^3/m^3, 0.014 m^3/m^3, and 0.010 m^3/m^3, respectively (Figs. 4.13, 4.14, & 4.15).

The destructive nature of soil sample collection for determining the VWC affects the accurate determination of the VWC. This affected the sensors at 20 cm depth compared to the deeper ones at 40 cm. The soil at the shallower depth is more likely to develop an air gap than the deeper sensors. The accuracy was found to be better at a lower VWC (< 0.3) compared to the high VWC (Figs. 4.14 & 4.15).

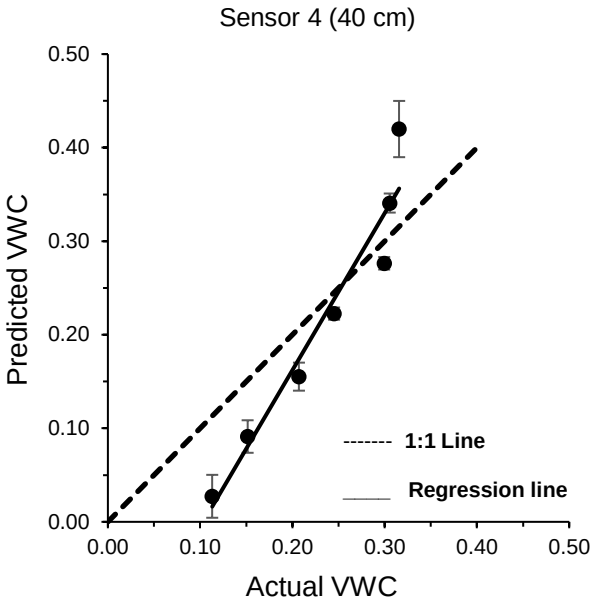

Fig. 4.16 Field validation of sensor_4

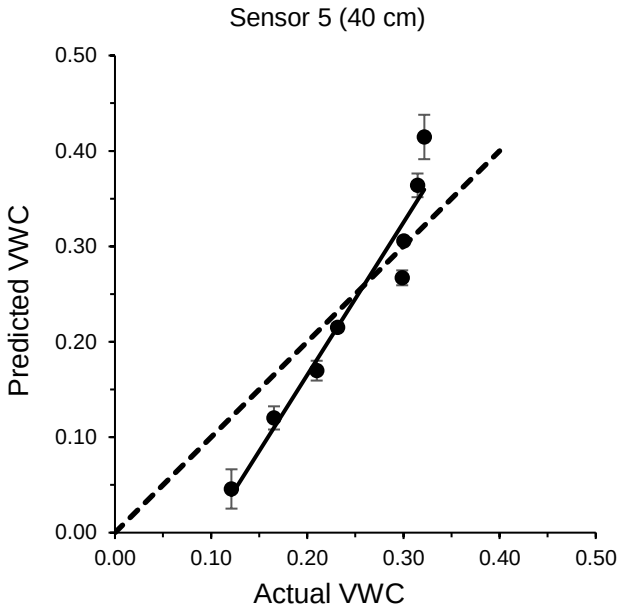

Fig. 4.17 Field validation of sensor_5

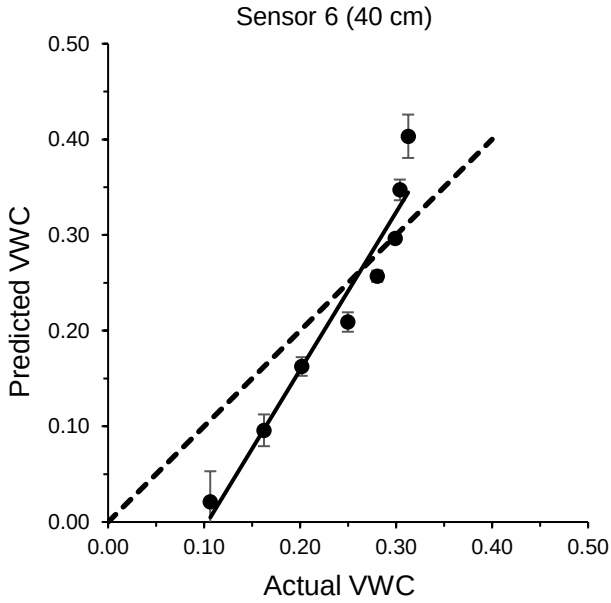

Fig. 4.18 Field validation of sensor_6

The accuracy of the predicted VWC was found to be low for all three sensors. The sensors were more accurate in the VWC range between 0.20 m^3/m^3 and 0.30 m^3/m^3.

The average standard error for the sensor_4, sensor_5, and sensor_6 was found to be 0.014 m^3/m^3, 0.01 m^3/m^3, and 0.01 m^3/m^3 respectively (Figs.4.16, 4.17, and 4.18). The method of installation of the sensor affects the sensor's performance (Iwata et al. 2017b). At 40 cm depth, the soil would be denser than the 20 cm layer. Even though surface contact of the sensor with soil improves the performance, higher compaction developed during the installation leads to low accuracy of the VWC values (Rothe et al. 1997).

Packing the soil well around the sensor without disturbing the physical characteristics and monitoring the air gap between the sensor and the soil would improve the performance of the sensor with better accuracy and precision.

4.6 Comparison of SEN0193 Sensor's Performance with TEROS T10 sensors.

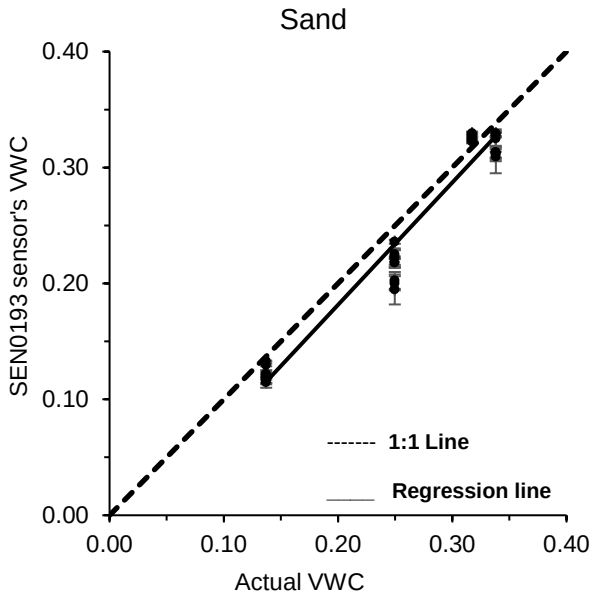

Fig. 4.20 Performance of SEN0193 sensor in sand

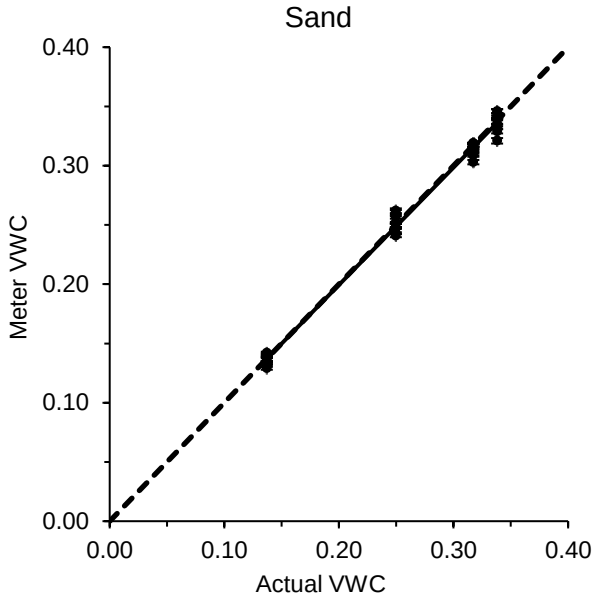

Fig. 4.19 Performance of Meter sensor in sand

Four different VWC samples were prepared for each soil texture, and their actual VWC was measured using the gravimetric method. Each of the actual VWCs was plotted against the VWC measured by the two types of sensors, as shown in Figs. 4.19, 4.20, 4.21, 4.22, 4.23, & 4.24. The temperature was set to 22^0 C during the study.

T10 sensors performed better in the sand, demonstrating good accuracy by closely following the 1:1 line and good precision with smaller error bars. As in Fig. 4.20, the regression line did not deviate from the 1:1 target line. The average standard error in predicting the VWC from the T10 sensor was 0.001 m^3/m^3. Compared to the SEN0193 sensors, the T10 sensors have a sharper probe, which enables better installation and maximum surface contact of soil around the probe. The SEN0193 sensors underpredicted the VWC by 0.02 m^3/m^3 with slightly lower precision exhibited by the larger error bars than the T10 sensors (Fig. 4.19).

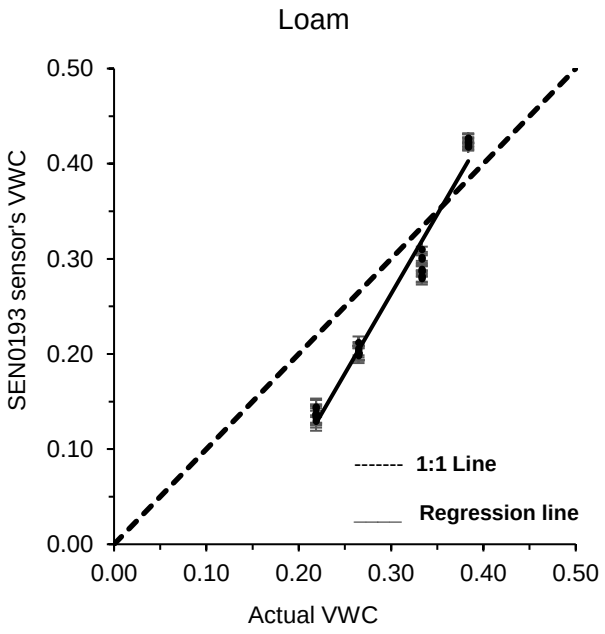

Fig. 4.24 Performance of SEN0193 sensor in loam

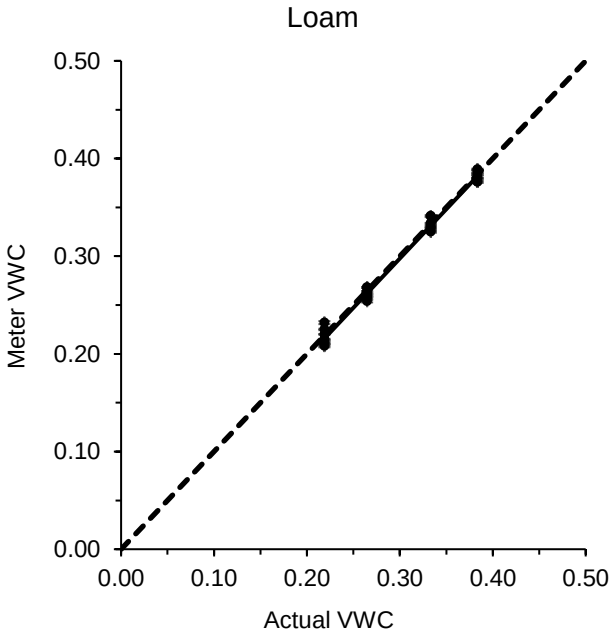

Fig. 4.21 Performance of Meter sensor in loam

The accuracy of the SEN0193 was poor in the loam soil except near the VWC of 0.317 m^3/m^3. The T10 sensors performed well in loam samples with better accuracy and precision. Smaller error bars indicate that the precision of the T10 sensors was better than SEN0193 sensors (Fig. 34.21).

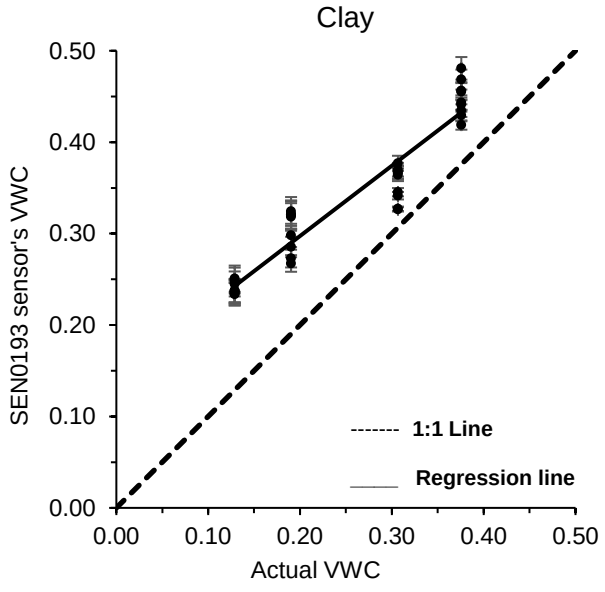

Fig. 4.23 Performance of SEN0193 sensor in clay

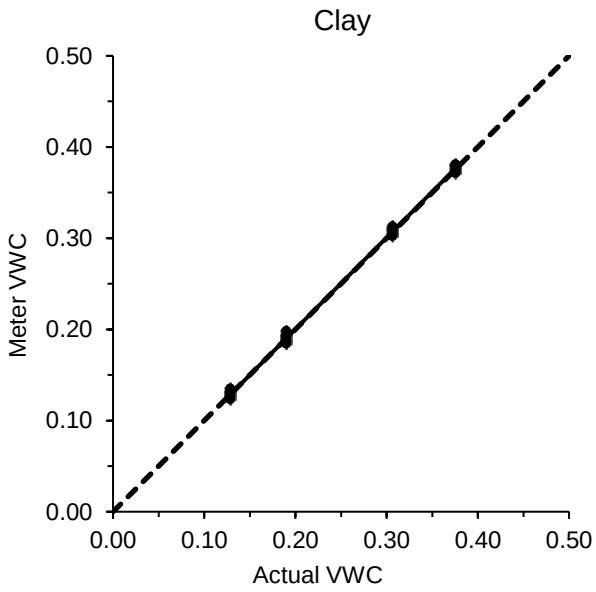

Fig. 4.22 Performance of METER sensor in clay

Compared to the robust design of T10 sensors, SEN0193 sensors need to be embedded carefully without disturbing the soil's physical properties, which affects the sensor's performance significantly. The lack of soil contact around the sensor or even higher compaction during the installation leads to poor accuracy of the sensors.

As in Fig. 4.23, the SEN0193 sensor responded poorly with clay samples. All the VWC values were overpredicted with poor accuracy and precision compared to the T10 sensor. The T10 sensors performed well in clay soils than loam and sand samples with a lower average standard error of 0.0004 m^3/m^3 (Fig, 4.24). Among the three-soil texture type, SEN0193 sensors demonstrated a higher error value of 0.01 m^3/m^3 in clay.

4.7 Root water uptake pattern on canola in Winkler study field.

The SEN0193 sensors were installed in a mature crop with a well-developed root zone. Winker weather data was obtained from the nearest weather station in Morden, MB. During the study period of August 13 to September 20, 2021, rainfall events were recorded on six different days (Fig. 4.25).

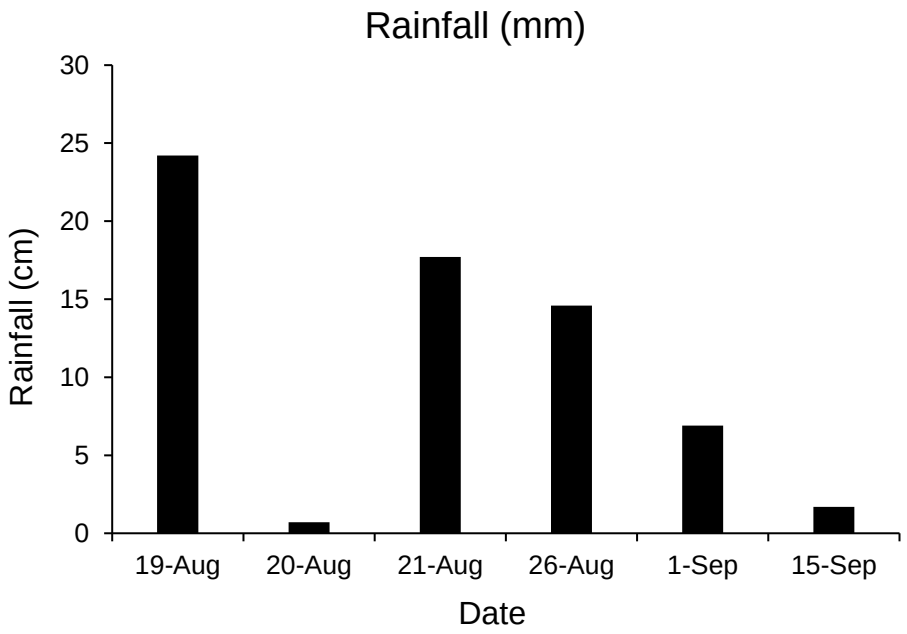

Fig. 4.25 Precipitation recorded on Winkler

The maximum amount of rainfall (24.2 mm) was recorded on August 19, 2021, and the minimum amount of rainfall (0.7 mm) was recorded on August 20, 2021. Water movement around the root zone can be effectively interpreted with rainfall data. The recorded sensor values were converted to the respective VWC values by using the calibration equation for the loam soil at Winkler. Twelve sensors were placed as an array in the vertical orientation to generate the volumetric water content contours, as shown in the following fig. 4.26. Contour plots were generated using the Sigma plot software to interpolate the point data into VWC contour maps in the vertical plane (Figs. 4.27, 4.29, 4.31, 4.33, 4.35, and 4.37).

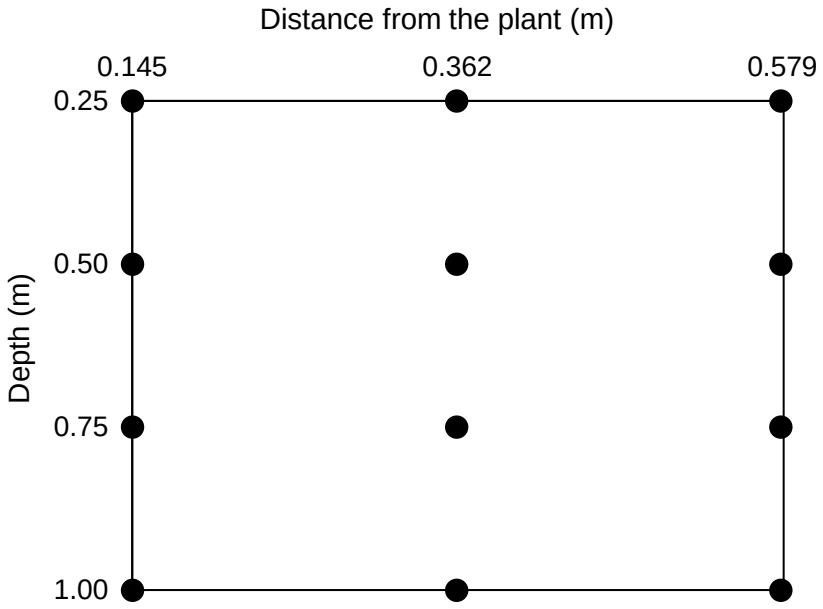

Fig. 4.26 Sensor arrangement of on the root zone

The VWC contour graphs are snapshots of water movement within the rootzone showing the spatial distribution of the water content for Morning (08:00 – 10:00), Afternoon (13:00 – 15:00), and Late evening (17:00 – 19:00). The VWC vs. depth curves at three different periods during day are plotted to understand the water flux within the root zone on that day.

On August 13, 2021, when water was applied as irrigation, it did not infiltrate through the soil deep because the soil profile was dry. As shown in Fig. 4.27, the plant consumed some of the water applied as irrigation as ET on that day. Since water content was depleted near the surface as the day progressed, the soil became drier in the late evening. Fig. 4.28 shows that soil was wet up to 50 cm depth, then water started to move into the deep layer of 100 cm and contributed to a slight increase of 0.03 m^3/m^3 water content at the end of the day.

Even though the moisture content of the field was observed for six weeks, significant changes occurred during the rainy days of August 20, 22, and 27 and September 2 and 16.

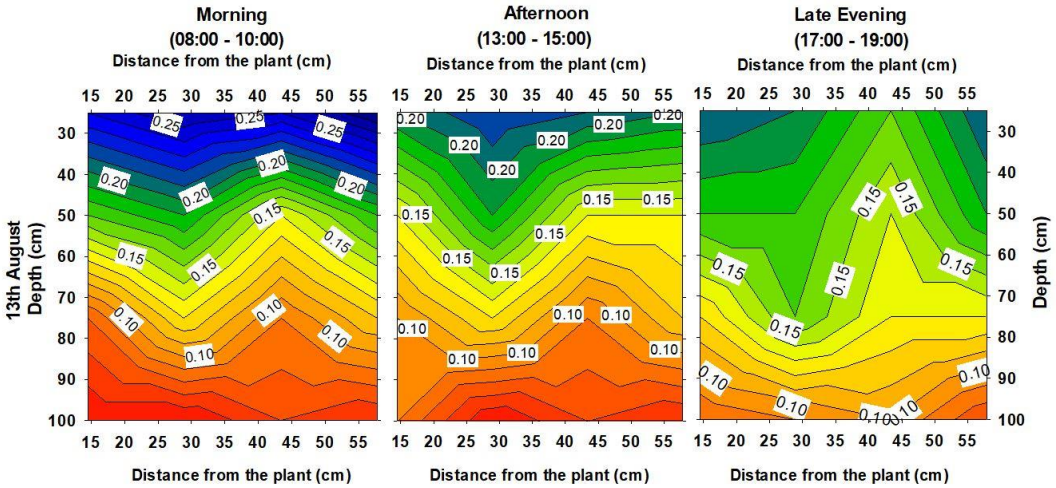

Fig. 4.30 Contour map of VWC on 13th August

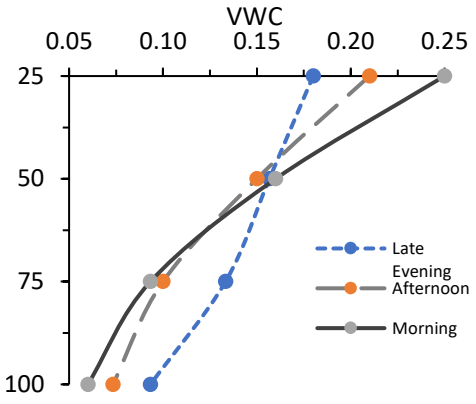

Fig. 4.28 Water movement in the root zone

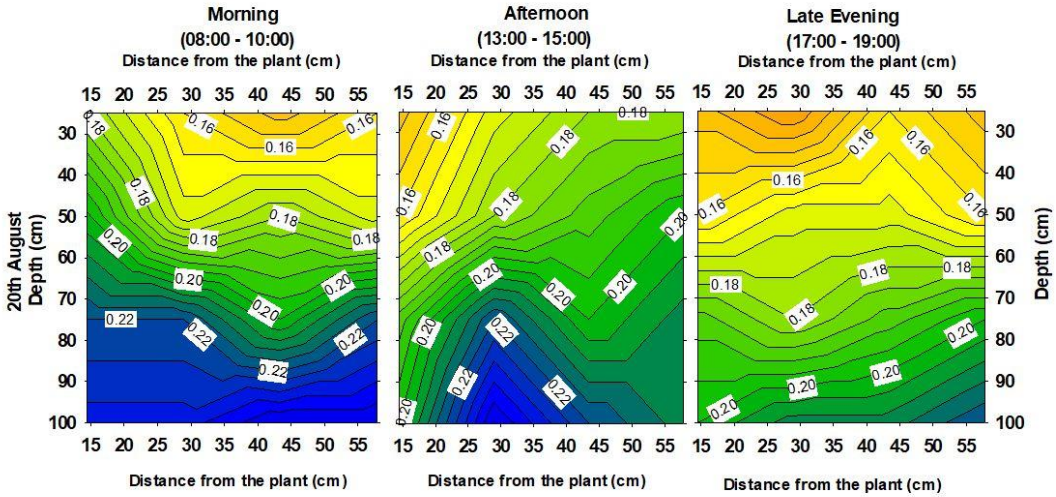

Fig. 4.29 Contour map of VWC on 20th August

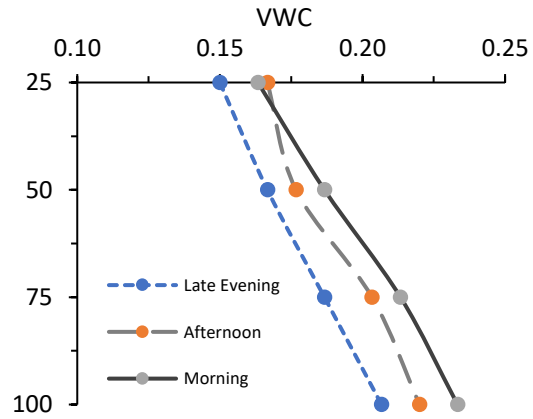

Fig. 4.27 Water movement in the root zone

After the rainfall event on August 19, 2021 (Fig. 4.25), comparing the figs. (4.27) & (4.29), it was clear that upward groundwater flux occurred and made deep layers wet compared to the shallower layers on August 20, 2021. The rainwater infiltrating through the layers increased the water content, which led to higher hydraulic conductivity promoting the upward groundwater flux towards the root zone. Even though the surface layer water content remained dry in the morning, it slowly gained some VWC of 0.02 m^3/m^3 around the afternoon (Fig. 4.30). The upward flux of groundwater is cut back at the end of the day because of the lower soil water content caused by crop ET.

Due to the higher ET demand in the evening, the soil was relatively drier than in the morning and afternoon. As shown in Fig. 4.30, throughout the day, VWC within the root zone varied from 0.16 near the surface to 0.22 m3/m3 towards the deeper layers. Figs. 4.29 and 4.31 indicate that amount of rainfall (0.7 mm) had no significant influence on the VWC around the root zone.

On August 22, 2021, upward groundwater flux contributed water to the 70 to 100 cm layer (Fig. 4.31). The groundwater at the Winkler site contains salts that would affect the crop roots adversely (Satchithanantham et al. 2014). Water content around the 50cm and 75cm depths did not change much compared to the change in water content observed around the depths of 25 cm and 100 cm (Fig. 4.32).

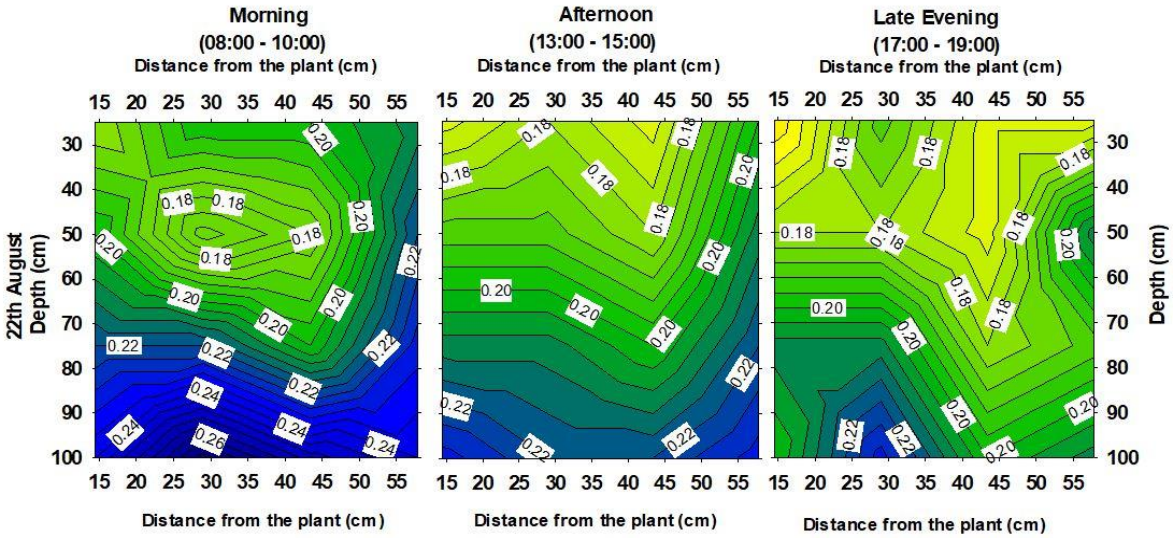

Fig. 4.32 Contour map of VWC on 22nd August

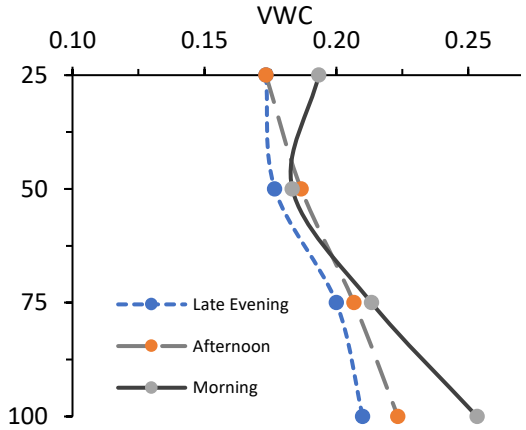

Fig. 4.33 Water movement in the Root zone

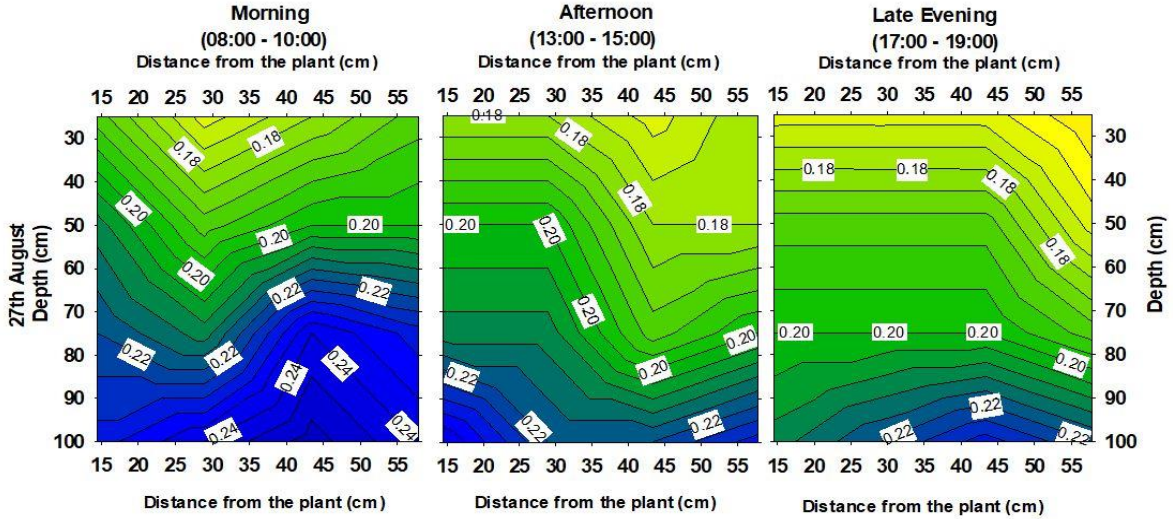

Fig. 4.34 Contour map of VWC on 27th August

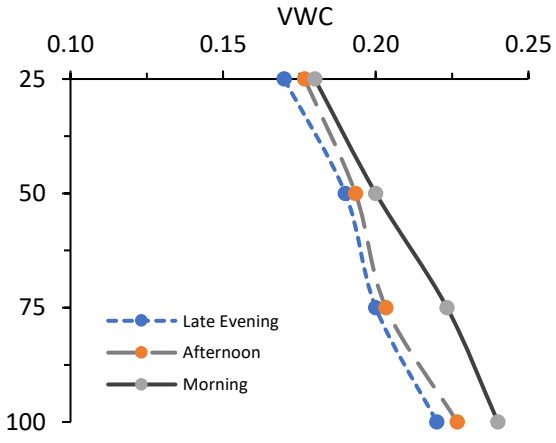

Fig. 4.31 Water movement in the Root zone

With the rainfall amount of 14.6 mm on August 26, 2021, upward groundwater flux reached a depth of 60 cm on August 27, 2021 (Fig. 4.33). The crop consumed this upward flux as ET. Over long-term saline water, upward flux to the root zone leads to a higher osmotic potential affecting plant water uptake. Deep-rooted crops like canola with shallow groundwater resources need to adopt good irrigation practices to remove the excess salt from within the root zone.

As shown in Fig. 4.34, water content on the surface layer (25 & 50cm) was retained at the same range for an extended period. In contrast, moisture movement from the morning to the afternoon at a depth of 75cm was found to be slightly higher. Overall, compared to the morning, by late evening, the VWC at 25, 50, 75, and 100cm changed by 0.1 m3/m3, 0.1 m3/m3, 0.2 m3/m3, and 0.2 m3/m3, respectively.

Groundwater upward flux was found to be higher up to 50 cm depth on September 2, 2021, like August 22, 2021(Fig. 4.35). Even with no rainfall for four days, the moisture around the root zone seems to be high, contributing to the higher hydraulic conductivity facilitating the upward flux of the groundwater to the shallower depth. The smaller pores within the wet soil act as a capillary and allows the water to rise (Radcliffe and Simunek 2010).

Fig. 4.36 shows that water movement varied vastly during the afternoon at each depth compared to the morning and late evening. Near the surface, the VWC depleted from 0.18 m3/m3 to 0.15 m3/m3 due to the ET of the crop. In the deep layer, the change in VWC is from 0.23 m3/m3 to 0.21 m3/m3.

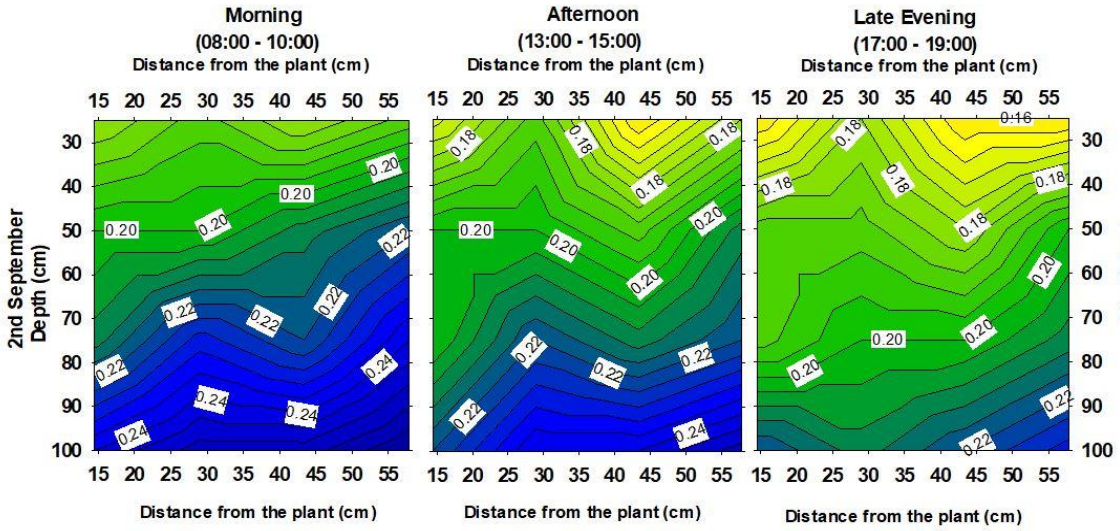

Fig. 4.35 Contour map of VWC on 2nd September

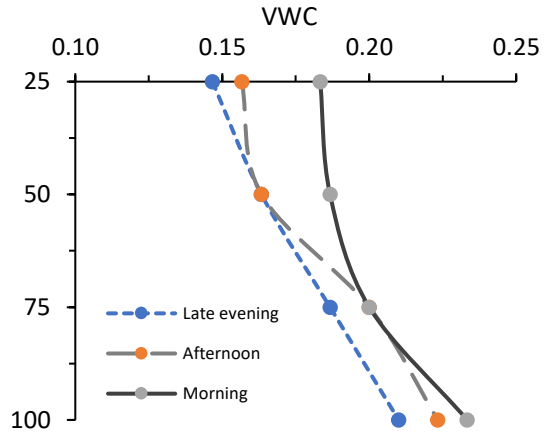

Fig. 4.36 Water movement in the Root zone

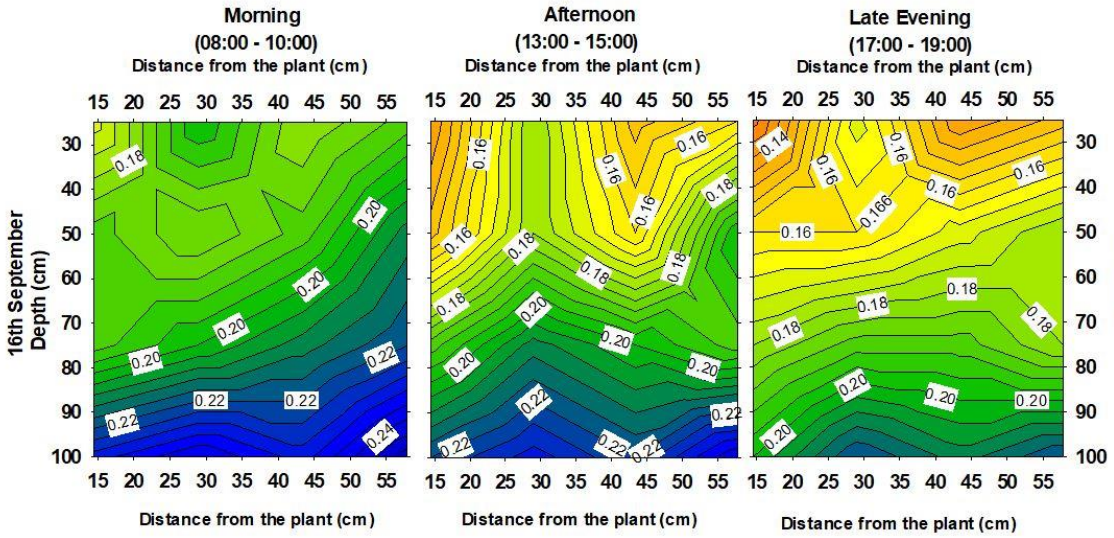

Fig. 4.38 Contour map of VWC on 16th September

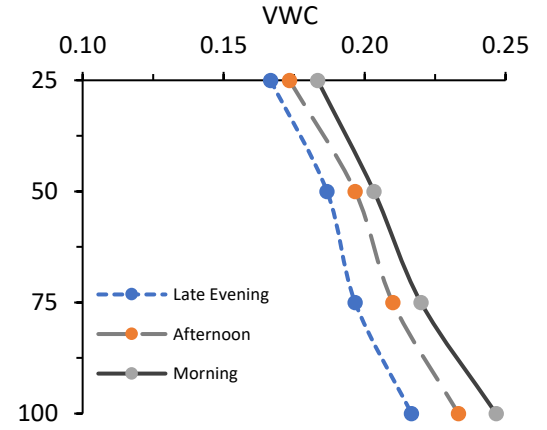

Fig. 4.37 Water movement in the Root zone

Canola was harvested from the study site on 5th September 2021. This significantly affected the water movement around the root zone area. On the 16th of September, upward groundwater flux was found to be very low compared to all other days (Fig. 4.37). With the low rainfall amount of 1.7 mm after 12 days, the drier soil had a decreased hydraulic connection to pull the groundwater upward. As the day progressed, the surface layer became dry in the afternoon because of soil water depletion to evaporation without the crop canopy after the harvest.

As shown in Fig. (4.38), at shallow depths (25 & 50 cm), the water content decreased by 0.1 m^3/m^3 from morning to late evening, while in the deeper layers (75 & 100 cm), the decrease was 0.2 m^3/m^3.

5.0 Conclusion

Three different soil calibration equations for three types of soils (Sand, Loam, and Clay) were developed for SEN0193 sensors under controlled laboratory conditions. The equations developed from the calibration of sensors demonstrated a good correlation of 91% for all three texture types. Performance could be increased by avoiding airgap between the sensor and the soil. The fragile design of the sensor needs careful installation. The calibration equation for sand performed better than for loam (0.003 m^3/m^3) and clay (0.003 m^3/m^3) with a precision of 0.002 m^3/m^3. The higher specific surface area of clay and its impact on the dielectric properties significantly affected the sensor performance. The validation of each sensor's performance is an indication of the performance of the developed calibration model in terms of accuracy and precision. Statistical parameters derived for each calibration model were in the acceptable range. Performance comparison of TEROS T10 sensors with SEN0193 sensors showed that the TEROS T10 sensor had better accuracy and precision. The RMSE values of Sand, Loam, and Clay were 0.022 m^3/m^3, 0.043 m^3/m^3, and 0.035 $m^3/m^{3,}$ respectively. The MBE indicated that the loam (-1.95E-16 m^3/m^3) and sand (-4.05E-15 m^3/m^3) calibrations were over predicting but clay (5.92E-15 m^3/m^3) calibration model was under predicting. The SEN0193 sensor was used to study the water uptake pattern of the canola at the Winkler study site. The water uptake pattern study within the canola root zone showed that the presence of crops influences the soil water movement by changing the soil water content. Higher hydraulic conductivity found during the rainfall influenced the upward groundwater flux. A shallow groundwater table with higher saline content affects the crop and leads to lower yield. This excessive water around the root zone must be drained to protect the crop.

6.0 Recommendations

Apart from the calibration, an in-depth study on the characteristics of SKU_SEN0193 sensors will help improve the sensor's performance and lead to more effective use of the sensor for larger field applications. Based on this study, the usefulness of the SKU_SEN0193 sensors can be broadened with the proper IoT instruments.

1. This study focused on developing better fitting calibration equations, including other components like the method of installation and packing of the soil without disturbing the physical properties, temperature, salinity, and pressure applied on the samples.
2. Root water uptake pattern observation can be improved using more sensors in the root zone in a three-dimensional way. Developing a 3D map of the root zone will help understand water movement in the root zone more precisely. Further modelling of the study site using hydrological software like Hydrus would help to understand the water movement within the soil in response to crop water use.

REFERENCE

Adelakun, I.A. 2013. Design of a Multilevel-TDR Probe for Measuring Soil Water Content. University of Manitoba, Winnipeg.

Buckingham, E. 1907. Studies on the movement of soil moisture.

Capacitive_Soil_Moisture_Sensor_SKU_SEN0193-DFRobot. 2015. *DF Robot*. https://wiki.dfrobot.com/Capacitive_Soil_Moisture_Sensor_SKU_SEN0193 (2022 /12/19)

Clarke Topp, G. and P.A.T. Ferré. 2002. 3.1 Water Content, 417–545. John Wiley & Sons, Ltd. https://doi.org/10.2136/sssabookser5.4.c19

Cordeiro, M.R.C.., V.. Krahn, R.S.. Ranjan and S. Sager. 2016. Water table contribution and diurnal water redistribution within the corn root zone. *Canadian Biosystem Engineering Journal* 57. https://doi.org/10.7451/CBE.2015.57.1.39.

Evett, S.R.., L.K.. Heng, P.. Moutonnet and M.L.. Nguyen. 2008. Field estimation of soil water content: A practical guide to methods, instrumentation, and sensor technology. In *International Atomic Energy Agency, Vienna, Austria.*, 39–54.

Fares, A.., F.. Abbas, D. Maria and A. Mair. 2011. Improved calibration functions of three capacitance probes for the measurement of soil moisture in tropical soils. *Sensors* 11: 4858–4874. https://doi.org/10.3390/s110504858.

Ferrarezi, R.S.., S.K.. Dove and M.W. van Iersel. 2015. An automated system for monitoring soil moisture and controlling irrigation using low-cost open-source microcontrollers. *HortTechnology* 25(1): 110–118.

Gardner, C.. . . K.., T.J.. Dean and J.D. Cooper. 1998. Soil water content measurement with a high-frequency capacitance sensor. *Journal of Agricultural Engineering Research* 71(4):

395–403.

Gardner, W.H. 1986. Water content. *Methods of Soil Analysis, Part 1: Physical and Mineralogical Methods* 5: 493–544. https://doi.org/10.2136/SSSABOOKSER5.1.2ED.C21.

Hanks, R.J. 1992. Water Quantities. In *Applied Soil Physics: Soil Water and Temperature Applications*, 1–22. https://doi.org/10.1007/978-1-4612-2938-4_1.

Hignett, C.. and S. Evett. 2008. Direct and surrogate measures of soil water content. In *Soil and Water Management and Crop Nutrition Section*, 1–22.

Hua, Y.., T.. Zejun, X.. Zhen, G.. Dingneng and H. Haoxing. 2016. Design of soil moisture distribution sensor based on high-frequency capacitance. *International Journal of Agricultural and Biological Engineering* 9(3): 122–129. https://doi.org/10.3965/j.ijabe.20160903.2226.

Iwata, Y., T. Miyamoto, K. Kameyama and M. Nishiya. 2017a. Effect of sensor installation on the accurate measurement of soil water content. *European Journal of Soil Science* 68(6): 817–828.

Ju, Z.., X.. Liu, T.. Ren and C. Hu. 2010. Measuring soil water content with time domain reflectometry: An improved calibration considering soil bulk density. *Soil Science* 175(10): 469–473.

Kahimba, F.C., R. Sri Ranjan, J. Froese, M. Entz and R. Nason. 2008. Cover crop effects on infiltration, soil temperature, and soil moisture distribution in the Canadian prairies. *Applied Engineering in Agriculture* 24(3): 321–333. https://doi.org/10.13031/2013.24502.

Kaja, K.P. 2017. HYDRUS modelling to predict field trafficability under different drainage design and weather conditions in Southern Manitoba. University of Manitoba, Winnipeg.

Livingston, B.E. 1908. A method for controlling plant moisture. In *Plant World*, 39–40.

Malmberg, C.G. and A.A. Maryott. 1956. Dielectric constant of water from 0 to 100 C. *Journal of Research of the National Bureau of Standards* 56(1): 1–8.

Mkhabela, M.S. and P.R. Bullock. 2012. Performance of the FAO AquaCrop model for wheat grain yield and soil moisture simulation in Western Canada. *Agricultural Water Management* 110: 16–24.

Nagahage, E.A.A.D., I.S.P. Nagahage and T. Fujino. 2019. Calibration and validation of a low-cost capacitive moisture sensor to integrate the automated soil moisture monitoring system. *Agriculture* 9(7): 141.

Ndulue, E. and S.R. Ramanathan. 2022. DRAINMOD simulation of drain spacing impact on canola yield in heavy clay soils in the Canadian prairies. *Irrigation and Drainage* 71(3): 711–727. https://doi.org/10.1002/IRD.2683

Nolz, R.., G.. Kammerer and P. Cepuder. 2013. Calibrating soil water potential sensors integrated into a wireless monitoring network. *Agricultural Water Management* 116: 12–20.

Placidi, P.., L.. Gasperini, A.. Grassi, M.. Cecconi and A. Scorzoni. 2020. Characterization of low-cost capacitive soil moisture sensors for IoT networks. *Sensors* 20(12): 3585.

Proulx, S. 2001. Evaluation of the performance of soil moisture sensors in laboratory-scale lysimeters. University of Manitoba, Winnipeg.

Radcliffe, D.E. and J. Simunek. 2010. *Soil Physics with Hydrus_ Modeling and Applications*. 1st editio. CRCpress. https://doi.org/https://doi.org/10.1201/9781315275666.

Radi, Murtiningrum, Ngadisih, F.S. Muzdrikah, M.S. Nuha and F.A. Rizqi. 2018a. Calibration of Capacitive Soil Moisture Sensor (SKU:SEN0193). In *Proceedings - 2018 4th International Conference on Science and Technology, ICST 2018*, 1–6. https://doi.org/10.1109/ICSTC.2018.8528624.

Roth, K., R. Schulin, H. Flühler and W. Attinger. 1990. Calibration of time domain reflectometry for water content measurement using a composite dielectric approach. *Water Resources Reserach* 26(10): 2267–2273. https://agupubs.onlinelibrary.wiley.com/doi/abs/10.1029/WR026i010p02267

Rothe, A., W. Weis, K. Kreutzer, D. Matthies, U. Hess and B. Ansorge. 1997. Changes in soil structure caused by the installation of time domain reflectometry probes and their influence on the measurement of soil moisture. *Water Resources Research* 33(7): 1585–1593. https://doi.org/10.1029/97WR00677.

Rowlandson, T.L.., A.A.. Berg, P.R.. Bullock, E.. Rotimi Ojo, H.. Mcnairn, G.. Wiseman and M.H. Cosh. 2013. Evaluation of several calibration procedures for a portable soil moisture sensor. *Journal of Hydrology* 498: 335–344. https://doi.org/10.1016/j.jhydrol.2013.05.021.

Rudnick, D.R.., K.. Djaman and S. Irmak. 2015. Performance analysis of capacitance and electrical resistance-type soil moisture sensors in a silt loam soil. *Transactions of the ASABE* 58(3): 649–665.

Ruelle, P.. and J.P. Laurent. 2008. CS616 (CS615) water content reflectometer. In *Soil and Water Management and Crop Nutrition Section*, 101–111. International Atomic Energy Agency.

Satchithanantham, S., V. Krahn, R. Ranjan and S. Sager. 2014. Shallow groundwater uptake and irrigation water redistribution within the potato root zone. *Agricultural Water Management* 132: 101–110.

da Silva, T.J.A.., E.M.. Bonfim-Silva, A.B.. Pacheco, T.F.. Duarte, H.H.. de Freitas Sousa and J. V. jose. 2018. Evaluation of various soil moisture sensors in four different soil types. *Applied Engineering in Agriculture* 34(6): 963–971. https://doi.org/10.13031/aea.12712.

Smith-Rose, R.L. 1933. The electrical properties of soil for alternating currents at radio frequencies. In *Proceedings of the Royal Society of London. Series A, Containing Papers of a Mathematical and Physical Character*, 359–377. The Royal Society. https://doi.org/10.1098/RSPA.1933.0074.

Stalham, M.A.. and E.J. Allen. 2004. Water uptake in the potato (Solanum tuberosum) crop. *The Journal of Agricultural Science* 142(4): 373–393. https://doi.org/10.1017/S0021859604004551.

Starr, J.L.. and I.C. Paltineanu. 2002. Methods for measurement of soil water content: Capacitance devices. *Methods of Soil Analysis: Part, 4*.

TEROS 10 Support | METER Group, Inc. USA. 2018. *Meter Environment*. https://www.metergroup.com/en/meter-environment/products/teros-10/teros-10-support (2022 /12/19)

Topp, G.. C.. and P.A. Ferre. 2002. The soil solution phase. In *Methods of Soil Analysis: Part.4*, 417–1074.

Topp, G.C.., J.L.. Davis and A.P. Annan. 1980a. Electromagnetic determination of soil water content: Measurements in coaxial transmission lines. *Water Resources Research* 16(3): 574–582. https://doi.org/10.1029/WR016I003P00574.

Topp, G.C. and P.A.T. Ferré. 2002. Water Content. In *Methods of Soil Analysis, Part 4: Physical Methods*, 417–545. https://doi.org/10.2136/SSSABOOKSER5.4.C19.

Topp, G.C. and T.P. Ferré. 2005. Measuring Soil Water Content. *Encyclopedia of Hydrological Sciences* 6. https://doi.org/10.1002/0470848944.HSA076.

Yoder, R.E.., D.L.. Johnson, J.B.. Wilkerson and D.C. Yoder. 1998. Soilwater sensor performance. *Applied Engineering in Agriculture* 14(2): 121–133.

Yu, C., A.W. Warrick, M.H. Conklin, M.H. Young and M. Zreda. 1997. Two-and three-parameter calibrations of time domain reflectometry for soil moisture measurement. *Water Resources Research* 33(10): 2417–2421. https://doi.org/10.1029/97WR01699.

Yu, X.., X.. Yu, B.. Zhang and N. Liu. 2010. Comparison study of three common technologies for freezing-thawing measurement. *Advances in Civil Engineering* 2010: 10. https://doi.org/10.1155/2010/239651.